Photochemistry and Photobiology, 2011, 87: 82–102

The Photochemistry of Uracil: A Reinvestigation

Martin D. Shetlar* and Vladimir J. Basus§

Department of Pharmaceutical Chemistry, School of Pharmacy, University of California, San Francisco, CA

Received 29 June 2010, accepted 18 September 2010, DOI: 10.1111/j.1751-1097.2010.00826.x

ABSTRACT

Results from a re-examination of the photochemical reactions undergone by uracil (Ura) are presented. Irradiation of Ura in frozen aqueous solution at −78.5°C produces two diastereomeric (6-4) products, namely the *cis* and *trans* isomers of 5-hydroxy-6-4′-(pyrimidin-2′-one)-5,6-dihydrouracil. Upon heating in 0.1 M HCl, each of these compounds decomposes to form 6-4′-(pyrimidin-2′-one)uracil. In addition, evidence for production of a hydrate of a trimer of Ura is presented, Irradiation of this compound at 254 nm forms Ura and a (6-4) adduct as products. The compounds 5-4′-(pyrimidin-2′-one)uracil and 6-hydroxy-5,6-dihydrouracil were also present after Ura was irradiated in frozen aqueous solution. Cyclobutane dimers (CBDs) are formed when Ura is irradiated in the frozen aqueous state, in fluid aqueous and acetonitrile solution and in the presence of photosensitizers (*e.g.* acetone). Published information, concerning the identity and relative quantitative importance of the four CBD isomers (*cis-syn*, *cis-anti*, *trans-syn* and *trans-anti*) formed in these photochemical systems, is incomplete and often in substantial disagreement. Using chemical methods in conjunction with HPLC, the identity and relative amounts of the four dimers have been determined in each of these systems. Consequently, a number of inconsistencies found in the literature concerning dimer product identity and quantitative distribution have been resolved.

INTRODUCTION

The photochemistry of uracil (Ura), one of the nucleobases found in RNA and occasionally in DNA, has received considerable attention over the past 50 years. (For comprehensive reviews of nucleic acid photochemistry, as well as that of nucleobases, nucleosides, nucleotides, dinucleotides and oligonucleotides, see [1,2]; for reviews of more recent work, see [3,4]). One reason for this interest in Ura photochemistry is that it is one of the four main nucleobases found in cellular RNA. Photodamage to such RNA (*e.g.* messenger RNA) can have consequences for cellular function, particularly with respect to functions involving protein synthesis (5). However, photoreactions in RNA can also be used to gain information about structural aspects of RNA, say in the context of ribosomes (see, *e.g.* Zhirnov and Wollenzien (6) and references therein). The presence of Ura in the genomes of RNA viruses implies that photoreactions of Ura must be considered in studies of UV-induced genetic damage, such as inactivation of infectivity (see, *e.g.* Smirnov *et al.* [7]).

The main photoreactions that Ura undergoes in the absence of external additives lead to production of CBDs and a photohydrate. Four CBDs are formed, namely the *cis-syn* (*c,s*), *cis-anti* (*c,a*), *trans-syn* (*t,s*) and *trans-anti* (*t,a*) stereoisomers (8) (displayed as **Ia**, **Ib**, **Ic** and **Id** in Scheme 1) while photohydration (9) yields 6-hydroxy-5,6-dihydrouracil (**II** in Scheme 1). Similar types of photoproducts are formed by the two other major nucleobases, cytosine and thymine (Thy) (for reviews, see [1,2,8–10]), while the *c,s*, *c,a* and *t,s* CBDs of 5-methylcytosine, a minor base occurring in mammalian DNA, have also been isolated and characterized (11). Analogous photohydration and photodimerization reactions have been observed when Ura is incorporated into nucleosides, nucleotides, oligonucleotides, polynucleotides and nucleic acids (for reviews, see [1,2,8–10]). A number of other studies have looked at the photoinduced reactions of Ura with species added to its aqueous environment. Among the reactions for which products have been isolated and characterized are those resulting from photo-induced reaction of this compound with hydrogen cyanide in aqueous solution (12), alcohols (see [13,14] for reviews), amines (15) and the amino acid cysteine (16). Survey studies have suggested that Ura, either as a nucleobase (17) or when incorporated into polyuridylic acid (18), is reactive with a number of amino acids other than cysteine.

Another type of reaction that appears to be characteristic of the pyrimidine bases, either when irradiated in the frozen state as the nucleobase or nucleoside or when incorporated into dinucleotides, oligonucleotides and nucleic acids and irradiated in solution, is formation of so-called (6-4) adducts (for reviews, see [1,2,19]). The photoreaction of Ura (or related compounds) to form a corresponding (6-4) adduct, namely 5-hydroxy-6-(4′-pyrimidin-2′-one)-5,6-dihydrouracil (see, *e.g.* structure **IIIa**) has not been directly demonstrated. However, the occurrence of this reaction has been inferred through the identification of a putative dehydration product, 6-4′-(pyrimidin-2′one)uracil (**IV**) (20). It has been generally assumed that the parent (6-4) adduct is very labile, undergoing fast spontaneous dehydration to form **IV** ([19], p 333). As acid hydrolysis of one of the chromatographic fractions obtained in the study of the photoreaction of uridine in frozen aqueous solution produced material with the properties of **IV**, Varghese

§Current address: Vladimir J. Basus, Caixa Postal 007, Extrema, Minas Gerais 37640-006, Brazil.

*Corresponding author e-mail: shetlar@cgl.ucsf.edu (Martin D. Shetlar)

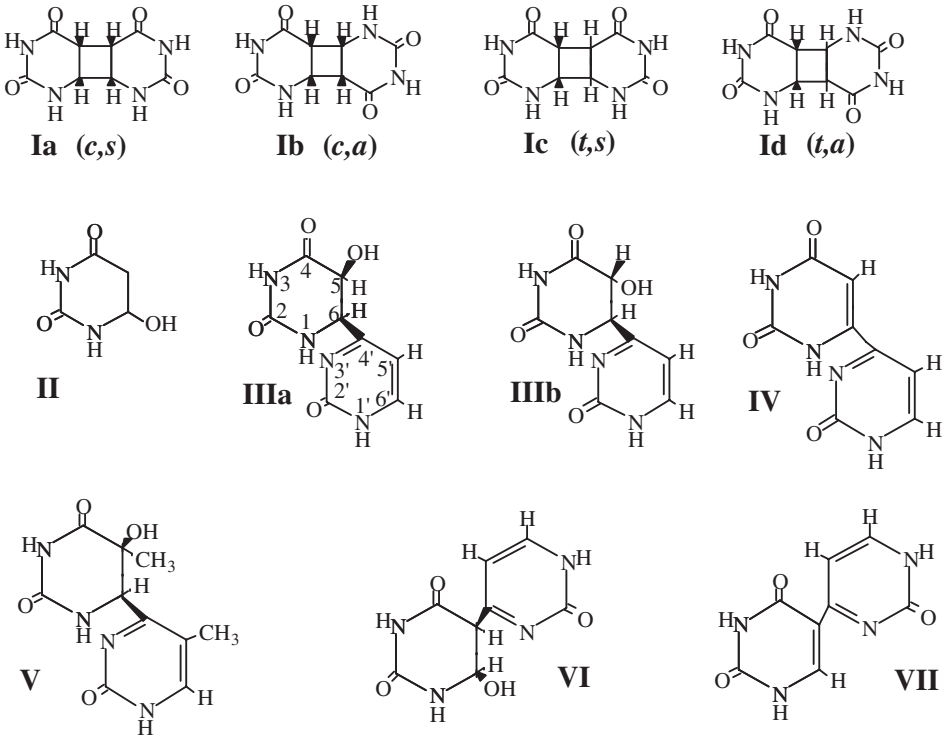

Scheme 1.

(21) concluded that a precursor (6-4) adduct is formed in this system as well.

In spite of the extensive previous work done on the photochemistry of Ura itself, there are a number of outstanding questions. One of these questions concerns whether a Ura (6-4) adduct would be sufficiently stable to allow its isolation and characterization. A second question deals with unresolved issues in the literature concerning the identity and quantitative distribution of the CBDs of Ura formed in various photochemical reaction systems. As pointed out in 1976 by Fisher and Johns (8) (pp. 248–252), there are significant disagreements in the literature concerning these matters, both in directly induced reactions (*i.e.* in ice and in fluid solution) and in reactions photosensitized by acetone; since that time, there have been no published reports that resolve these contradictions.

In this paper, we show that two isomeric (6-4) adducts of Ura can be isolated and characterized after this nucleobase is irradiated in the frozen aqueous state. In addition, we have looked in detail at the products of the Ura photodimerization reactions occurring in four systems, namely in fluid aqueous and acetonitrile solution, in frozen aqueous solution and when the photoreactions of Ura are sensitized by acetone in aqueous solution. Using chemical methods, we have definitively established the identities of the dimers formed and, using HPLC, we have studied the quantitative distribution of the four CBDs (*c,s*, *c,a*, *t,s* and *t,a*) formed in each of these four systems. These results provide a considerably more complete description of the photochemical reactions occurring in these systems than has been previously available. They also resolve a number of contradictions found in the literature.

MATERIALS AND METHODS

General Aspects. Uracil and Thy were obtained from Sigma (St. Louis, Mo). HPLC solvents were from Fisher (Fair Lawn, NJ), while NMR solvents were provided by Aldrich (Milwaukee, WI). Chemicals used in various methylation procedures were from Aldrich. Preparative separations were accomplished on a Shiseido Capcell UG120 10×250 mm column (5 mm particle size, Yokohama, Japan) (Column A), while analytical HPLC separations were carried out using a Capcell UG120 4.6×150 mm column (5 mm particle size) (Column B), a Microsorb Phenyl column (4.6×250 mm, 5 mm particle size; Varian, Walnut Creek, CA) (Column C) and a Microsorb Amino column (4.6×250 mm, 5 μm particle size) (Column D). In some cases, final purification was done on Column C. Column E, used in some experiments, was a Capcell UG120 4.6×250 mm column (5 mm particle size). The HPLC system employed was a Rainin binary gradient pumping system (Emeryville, CA) coupled to a Hewlett-Packard 1040A diode array detector (Palo Alto, CA). Prior to injection, all HPLC samples were subjected to spin filtration on Costar Spin-X microcentrifuge tubes containing a 0.2 μm nylon filter (Corning Incorporated, Corning, NY). Rotatory evaporations were done on a Büchi R-200 Rotovapor (New Castle, DE) with vacuum provided by a mechanical pump; two dry ice traps were placed between sample and pump.

NMR spectra were run at 600 MHz on a Varian INOVA NMR spectrometer (Palo Alto, CA). MALDI mass spectra were obtained on an Applied Biosystems 4700 Mass Spectrometer (Foster City, CA), running in the reflector mode, while ESI mass spectra were run on either a Waters Micromass ZQ4000 instrument (Beverly, MA) or a Brucker Fourier Transform 9.4T spectrometer (Rheinstetten, Germany).

Unfiltered Spectronics BLE IT155 lamps, with output mainly at 254 nm and housed in Spectroline XX-15A lamp housings (Westbury, NY), were used for irradiations of Ura solution in the ice phase or to induce reaction in fluid aqueous solution; Spectronics BLE IT158 lamps, with output centered at 312 nm and contained in the same housing, were used to photosensitize reactions in solutions containing acetone.

Irradiations in the frozen state were done on 250 mL batches of aqueous Ura (2 mM). Each batch was placed in a 13 × 9 inch non-stick baking pan (Bradshaw International, Rancho Cucamonga, CA) and frozen on two 25 × 25 cm dry ice slabs (−78.5°C) placed side by side. During freezing the pan was covered with a 15 × 10 inch Pyrex baking dish, so as to minimize frosting of the surface of the frozen solution. Four lamps, contained in two Spectroline X-Series lamp housings, were placed on top of the pan containing the solutions; irradiation was done with the pan resting on the dry ice slabs. The exposure at the surface of the frozen aqueous layer in the pan averaged around 25 J m^{-2} s^{-1}, as measured using a Spectronics DM-254N UV Meter (Westbury, NY).

Irradiations of Ura contained in acetonitrile solution were carried out on a small scale. A 3 mL portion of parent solution was placed in a 12 mm diameter flat-bottomed cylindrical quartz tube (75 mm in length) with a 14/35 quartz taper seal outer joint fused to its end. The tube was than fitted with a T-shaped adaptor fitted with a 14/35 taper seal inner joint and two screw joints compatible with Mininert valves suitable for Reactivials (Pierce, Rockford, IL). The taper seal and one of the screw joints were attached to the ends of the top bar of the tee. After fitting the screw joints with Mininert valves, an 8 inch long needle (Wilmad, Buena, NJ) was inserted through the septum of the Mininert valve attached to the top bar of the tee and pushed to the bottom of the tube; a short bleed needle pierced the septum of the second valve. The sample was deoxygenated with 99.997% pure N_2. After needle removal and valve closure, the UV spectrum of the sample was measured using acetonitrile in the same tube as a blank. During irradiation, the sample was placed next to an unfiltered BLE IT155 lamps.

Irradiations involving direct absorption of light by Ura in aqueous fluid solution, or photosensitized reactions of Ura in aqueous solution containing acetone, were carried out as described in the on-line Supporting Information section, which contains a discussion of the preparation of the CBDs of 1,3-dimethyluracil.

Preparation and fractionation of the noncyclobutane dimer photoproducts produced by irradiation of Ura in aqueous frozen solution. In this section, we describe the steps used in workup of aqueous solutions of Ura irradiated on dry ice, with a primary focus on putative (6-4) adducts(s) and trimer hydrate.

Preparation, characterization and workup of solutions of Ura irradiated at dry ice temperature. In a typical experiment, 1 L of solution (2 mM) was irradiated in 250 mL batches for 60 min. After thawing, 150 μL of the resulting yellow-green solution was diluted to 3 mL, its UV spectrum was measured and the absorbance at 258 nm was determined; a similar measurement were made with the parent solution and it was estimated that about 62% of the parent Ura had reacted. The 20-fold diluted irradiated sample displayed absorbance to the red of the parent Ura peak with a maximum at 304 nm and an absorbance of 0.014. Using an approximate value for ε_{304} of 4900 as the molar absorption coefficient of uracil (6-4) adducts (based on an analogous value of ε_{316} for the corresponding thymine-thymine adduct ([19], p. 341), it was calculated that a total of about 57 μM of (6-4) product was present in the original irradiated 1 L of solution and that about 9% of the Ura consumed had been converted to such compounds. This corresponds to about 12.8 mg of total (6-4) product of MW 224 being produced by irradiation of 1 L of solution. Using relative areas of HPLC peaks corresponding to Ura, the percent conversion was calculated to be about 59%. The calculated conversion varies by a couple of percentage points from run to run, as might be expected for situations where the reflective properties of the surface of the frozen solution being irradiated may not be identical for each run.

The HPLC properties of freshly irradiated solution were examined using Column A. A representative analytical chromatogram from a 500 μL injection is shown in Fig. 1; this chromatogram was obtained using the following water/methanol gradient at a flow rate of 5 mL min^{-1}: 0 min, 0% MeOH; 4 min, 0%; 5 min, 15%; 8 min, 15%; 8.5 min, 0%; 14 min, 0%. The peaks labeled 2 and 3 elute with retention times corresponding to the putative (6-4) adducts of interest;

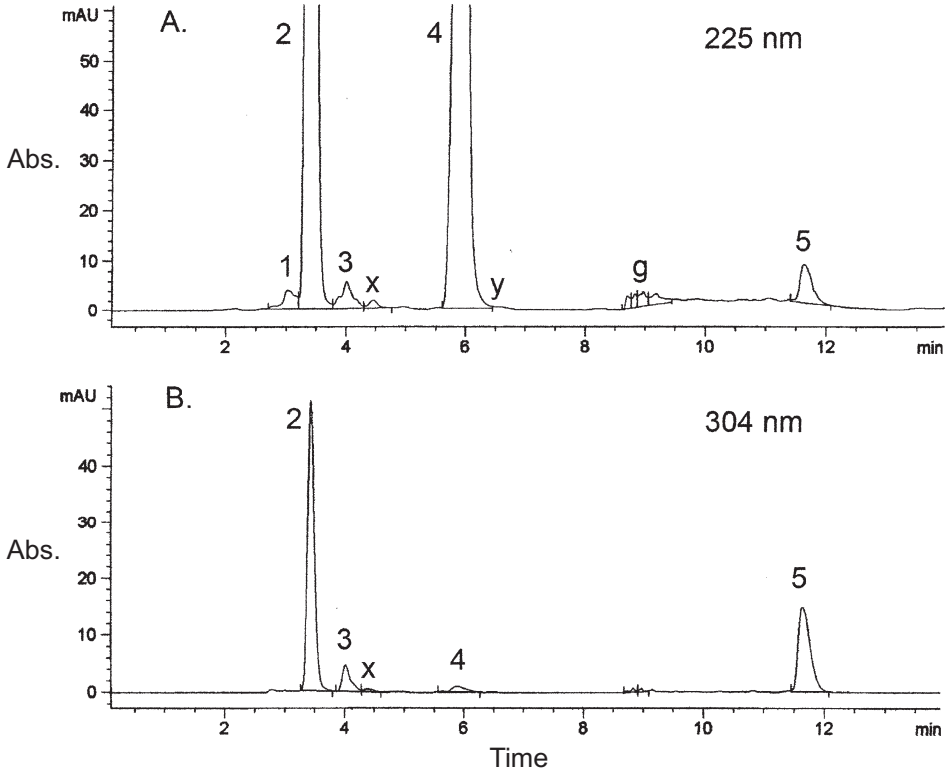

Figure 1. The HPLC chromatogram resulting from injection of 500 μL of a freshly prepared 2 mM solution of uracil that was frozen on dry ice and irradiated for 60 min as described in Materials and Methods. Panel A displays the chromatogram seen with detection at 225 nm, while panel B corresponds to that observed with detection at 304 nm. The chromatogram was obtained on a Shiseido Capcell UG120 10 × 250 mm column using the following water/methanol gradient at a flow rate of 5 mL min^{-1}: 0 min, 0% MeOH; 4 min, 0%; 5 min, 15%; 8 min, 15%; 8.5 min, 0%; 14 min, 0%. Detailed identification of the peaks is discussed in Materials and Methods; however, the peaks labeled 2 and 3 in Panel B correspond to (6-4) adducts.

however, the main type of product eluting in peak 2 is cyclobutane dimer in nature. Peak 4 corresponds to unreacted Ura, although CBD-type product coelutes with the parent compound. The materials corresponding to peaks 1, 2, 3 and 4 were the focus of the investigations described below. The material eluting in Peak 5 shows a UV spectrum with a broad absorption band centered at 313 nm; the spectrum and elution time are different than those of the previously characterized 6-4′-(pyrimidin-2′one)uracil (**IV**) (20). The compound responsible for this peak is lost during workup and was not characterized. The products responsible for the peaks denoted by x and y were likewise not identified in our studies of this reaction system. The complex of peaks denoted by g is artifactual and characteristic of the eluting gradient, being present even in the absence of injected sample.

The liter of irradiated solution was reduced to 20 mL by rotatory evaporation at 40°C, placed in the cold (8°C) overnight, and then filtered through a Whatman HAWP filter to remove the precipitated material (mostly Ura CBDs). This precipitate had a yellow-tan cast. The precipitate was washed with 5 mL of distilled water; the wash solution was added to the parent solution and, after appropriate dilution, this solution was assayed for (6-4) adduct by UV spectroscopy. About 85% of the material absorbing at 304 nm was recovered in this solution. A UV absorbing tail extending out to 375 nm was present in the original photolyzed solution, but not in the diluted assay sample; this suggests that one or more additional compounds contribute to the 304 nm absorbance in the original irradiated solution (see below for discussion of the nature of such compounds). Indeed, an HPLC assay indicated that about 97% of total putative (6-4) adduct remained in the concentrated solution. The 25 mL of concentrate was further concentrated to 3 mL by rotatory evaporation and filtered; the precipitated material was washed with five 1 mL portions of distilled water. The wash solution was added to the filtrate, along with an additional 2 mL of distilled water, to give a total of 10 mL of concentrated solution. An HPLC assay of this concentrate indicated that about 94% of the original putative (6-4) adducts had been recovered.

An alternate method for preparation of concentrates of Ura photoproducts. A modified approach was explored as an alternative for preparation of concentrates of putative (6-4) adducts from Ura solutions irradiated in ice. In a typical run using this procedure, 990 mL of solution, irradiated as described above, was concentrated to about 46 mL. The resulting concentrate was cooled on ice and filtered. The filtrate was then taken to dryness using rotatory evaporation and 10 mL of methanol was added. The precipitate was scraped from the sides of the evaporation flask and the resulting slurry was placed in a 15 mL Falcon plastic centrifuge tube. After centrifugation in a swinging bucket rotor, the supernatant was removed by decanting to give extract E1. This same procedure was repeated two times to give E2 and E3. Assay of the UV absorbance of each of these extracts at 304 nm, after 10-fold dilution with distilled water, indicated that the absorbances of the three extracts had a ratio of 81.5:14.5:4. HPLC analysis of the extracts using Column C (see above), after removal of methanol by rotatory evaporation, dissolution of the residue in water and filtration, indicated that much of the cyclobutane dimeric product had been removed and that the extracts contained the putative (6-4) products of interest; however, Ura was the predominant component of each extract. (The analytical gradient used was as follows: 0 min, 0% MeOH; 3.75 min, 0%; 6 min, 20%; 7.5 min, 20%; 7.8 min, 0%; 12 min, 0%, flow rate: 1.6 mL min^{-1}). This gradient has the desirable attribute that it is able to resolve the peak containing putative (6-4) adduct from the main cyclobutane dimer peak; however, it is unable to resolve the two putative (6-4) adducts. Comparative analysis of the solution prepared by the approach described in the previous section and the solution prepared by extraction indicated that the former contained about 2.5-fold more CBD, while the amounts of (6-4) adduct were almost identical. The material corresponding to Peak 1 in Fig. 1 is present in samples prepared by either approach.

First pass separation of components of the photoproducts produced when Ura is irradiated in frozen solution at dry ice temperature. The concentrate obtained using the first approach described above was chromatographed in 1 mL batches on Column A using the following water/methanol gradient with a flow rate of 5 mL min^{-1}: 0 min, 0% MeOH; 4 min, 0%; 5 min, 15%; 8 min, 15%; 8.5 min, 0%; 16 min, 0%. Six fractions were collected. Fraction 1 (F1) eluting between 2.3 and 3.4 min, contained material with little UV absorbance above 250 nm, while F2 (3.4–3.9 min) was a compound with a slight peak of UV absorbance with a maximum at 304 nm, similar to that expected for (6-4) type products; this fraction also contained a large amount of other material, found to be cyclobutane dimer. Fraction F3 (3.9–4.5 min) contained a second compound with (6-4) adduct-like absorbance, along with another compound without UV absorbance above 250 nm and F4 (4.5–5.6 min) contained several products present only in small amounts. The fraction F5 (5.6–6.6 min) contained Ura and F6 (6.6–16 min) contained a variety of compounds present in small amounts, including the known (6-4) dehydration product **IV**. We gave our initial attention to characterization of the compounds with (6-4)-like absorbance contained in F2 and F3 and the material contained in F1. The final purification and characterization of these compounds is described in Results and Discussion.

Preparations and procedures relevant to identification and quantitation of the cyclobutane dimers of Ura. A second focus in our study of the photochemistry of Ura was identification and quantitation of the CBDs formed when the parent compound was irradiated under several conditions. Our approach to establishing the identities of the various CBDs of Ura involved conversion of purified dimers into methylated forms that had previously been well characterized *via* work published in the literature. This approach requires that we have authentic samples of the various CBDs of 1,3-dimethyluracil (DMU) and 1,3-dimethylthymine (DMT). The methods used for preparing these dimers are appropriately modified and modernized versions of those already published in the literature; the details of these procedures are described in Supporting Information. We also required samples of the various mixed dimers of DMU and DMT and knowledge of the chromatographic and chemical behaviors of these various dimers. By extending the methodology originally developed by Taguchi and Wang (22,23), as described below, we were able to satisfy this need, as well as verify the identity of various DMU and DMT dimers. We then describe how this methodology was used to assign a stereochemical identity to each Ura CBD. Finally, we describe chromatographic conditions that permit separation and quantitation of the each of the Ura CBDs when produced under various conditions of interest. (It should be noted that, while the *c,s* and *t,a* isomers of the Ura CBDs exist as single *meso* forms, the corresponding *c,a* and *t,s* forms of the Ura CBDs are, in fact, racemic mixtures of two optical isomers. Consequently, the results presented below, say for the *t,s* CBD, in actuality pertain to the corresponding racemic mixture of optical isomers.)

Preparation of mixed DMU-DMT cyclobutane dimers and verification of the stereochemistry of the DMT cyclobutane dimers. To determine (or confirm) the stereochemistry of each of the DMT CBDs, as well as prepare a reaction mixture containing each of the corresponding mixed DMU-DMT dimers, we utilized a modified version of the C-methylation methodology described by Taguchi and Wang (22,23). (The preparation of the various DMU and DMT CBDs used in the following protocols is described in Supporting Information.)

A slurry containing 320 mg of Ag_2O per mL of N,N-dimethylformamide (DMF) was prepared and stored in a glass stoppered flask. To two samples of each of the four DMU dimers of known stereochemistry, each sample containing about 1 mg of purified dimer and enclosed in a 1.5 mL screw top plastic microcentrifuge tube (Sarstedt, Newton, NC), was added 260 μL of slurry and 140 μL of methyl iodide. After mixing on a vortex mixer (Fisher, Tustin, CA), the resultant slurry was placed on the top of a Labline Orbital Shaker (Melrose Park, IL) and agitated at ambient temperature; one sample was removed after 3.5 h and the second after 16 h. Immediately after removal from the shaker, 270 μL of the slurry was removed and diluted with 230 μL of DMF. The resultant slurry was filtered using a Costar nylon spin tube and the filtrate was placed in a 15 mL plastic centrifuge tube. To this tube was added 2.5 mL of $CHCl_3$; this resulted in immediate formation of a white precipitate. After shaking, the tube was centrifuged and the supernatant was decanted from the compacted precipitate at the bottom of the tube. The $CHCl_3$ layer was shaken with 1 mL of water; after separation of the layers, 0.5 mL of the $CHCl_3$ layer was removed and placed in the bottom of a 1.5 mL Sarstedt screw top microcentrifuge tube. This sample was taken to dryness *via* rotatory evaporation in two stages. The chloroform was removed on a water aspirator driven apparatus at room temperature

and then drying was continued at 60°C on the Büchi Rotovapor; this latter step removes most of the DMF remaining after the water extraction of the $CHCl_3$. (The procedure used here omits a step included in the previous protocols [22–24], namely treatment with aqueous sodium cyanide; we found the end results were the same without it.) During the rotatory evaporation, the Sarstedt tube was fitted to the taper seal 24/40 joint of an antiflash rotatory evaporator trap using a Fisherbrand Sav-It 16 mm tube closure pierced by several holes. (The top of this type of closure fits snugly inside the taper joint, while the bottom of the closure fits tightly around the screw portion of the microcentrifuge tube.) The dried material was dissolved in 0.5 mL of water and filtered through a spin tube. The resulting solutions were chromatographed on Column B using the following water/MeOH gradient (Gradient D) run at 2 mL min^{-1}: 0 min, 7% MeOH; 4 min, 7%; 6.5 min, 40%; 8 min, 40%; 8.3 min, 7%; 13 min, 7%. In line with a previous finding by Taguchi and Wang, we observed that the DMU *c,s* dimer is resistant to methylation to form a corresponding *c,s* DMT homodimer, even after 16 h of incubation. However, Taguchi and Wang also indicated that a mixed dimer was formed in the methylation reaction. In agreement with their observations, we found a peak, corresponding to the mixed *c,s* DMU-DMT dimer, that eluted at 8.2 min in the reaction mixture that had been run for 16 h. Each of the other DMU CBDs reacts to form both a DMT dimer and a mixed dimer. The retention times of the four DMU dimers, and of the various dimers formed in the methylation reactions of each of the DMU CBDs, are shown in Table 1; the HPLC conditions corresponded to those of Gradient D on Column B, as described above. These data confirm that the order of elution of the DMT dimers using Gradient D as being *c,s*; *c,a*; *t,s*; *t,a*; the same order of elution also holds for the DMU dimers and the mixed DMU-DMT dimers.

As a further confirmation that the *c,s*, *c,a* and *t,s* DMT dimers, isolated as described in Supporting Information, were assigned correctly, we methylated authentic samples of each of the corresponding CBDs of Thy. For this purpose, we used a modified version of the procedure described by Blackburn and Davies (25). We dried samples of each isomer, suspended the residue in 1 mL of 1 M NaOH (0.4 M NaOH in the case of the *c,a* dimer) and added 100 μL of dimethyl sulfate. The resulting heterogeneous mixture was heated in boiling water for about a minute, after which the solution was homogeneous. Then 0.5 mL of $CHCl_3$ was added and the solution was shaken, so as to extract the methylated dimer into the chloroform phase. About 0.4 mL of the organic phase was removed and taken to dryness by rotatory evaporation at 40°C. The residue was taken up in 500 μL of water and 50 μL was chromatographed on column B, using Gradient D as described previously. In each case, the methylated dimer eluted at the same time as the corresponding authentic DMT dimer, while the absorption spectrum of each dimer could be superimposed on that of its corresponding DMT dimer. These results provide additional evidence that the identities of the *c,s*, *c,a* and *t,s* dimers of DMT are correctly assigned. It should be noted that the predominant product resulting from action of dimethyl sulfate on the *c,a* Thy dimer under the above conditions was DMT; *c,a* DMT CBD was the dominant minor product. Small amounts of additional products, most likely incompletely methylated dimers (26), were formed in each of the methylation reactions. We also found, as observed previously (26), that the *t,a* cyclobutane dimer of Thy does not methylate to form the corresponding tetramethlylated dimer.

Table 1. HPLC retention times for the cyclobutane dimers of 1,3-dimethyluracil (DMU-DMU), 1,3-dimethylthymine (DMT-DMT) and the mixed dimers of DMU and DMT (DMU-DMT).

Dimer	DMU-DMU	DMU-DMT	DMT-DMT
c,s	5.5 min	8.2 min	8.7 min*
c,a	7.5 min	8.9 min	9.4 min
t,s	8.7 min	9.4 min	9.9 min
t,a	9.1 min	10.0 min	10.5 min

Retention times were measured from chromatograms obtained from runs on a Shiseido Capcell UG120 column (4.6 × 150 mm) using the following water/MeOH gradient flowing at 2 mL min^{-1}: 0 min, 7% MeOH; 4 min, 7%; 6.5 min, 40%; 8 min, 40%; 8.3 min, 7%; 13 min, 7%.

*The retention time of the *c,s* DMT dimer was determined using an authentic sample prepared as described in the Supporting Information accompanying the paper. This dimer is not formed when the c,s DMU dimer is methylated.

Methylation of the CBDs of Ura and identification of individual dimer stereoisomers. The CBDs of Ura have very low solubilities and are difficult to separate by HPLC (particularly the *c,s* and *c,a* isomers [**Ia** and **Ib**]). In addition, the *c,a* and *t,a* isomers (**Ib** and **Id**) are somewhat labile when heated in aqueous solution or treated with acid or base. These properties present challenges to the investigator desiring pure samples of these materials for identification by use of structural techniques (*e.g.* by IR or NMR spectroscopy). Although IR spectroscopy has been used to identify the various Ura dimers, based on comparison of the resultant spectra with those of a synthesized sample of each isomer, application of this technique has also led to contradictory identifications. It was for this reason that we developed an independent means of assigning the stereochemical nature of each dimer, namely identification of the products produced by methylating the various dimers using protocols based on those used by Taguchi and Wang (22,23) for methylation of the DMU dimers. Information resulting from the use of such methylation reactions provides three pieces of evidence pointing to the correct assignment of the structure of a particular dimer (two for the *c,s* isomer). For example, methylation of the Ura *t,s* dimer should yield a reaction mixture that, upon examination by HPLC, would contain compounds that eluted with retention times and UV spectral characteristics corresponding to those of the *t,s* DMU CBD, the *t,s* DMU-DMT dimer and the *t,s* DMT-DMT CBDs, as tabulated in Table 1.

Elad and coworkers (24) found that methylation of the *c,s* CBD of Ura to form the corresponding DMU dimer went smoothly when it was treated with silver oxide and methyl iodide in DMF. In our work we used the modified procedure, outlined above for C-methylation of DMU CBDs, to carry out a similar reaction on fractions containing isolated Ura dimers, or dimer mixtures, to form the corresponding DMU, DMU-DMT and DMT dimers. Once the identities of the individual dimers were established, we could quantitatively evaluate the distribution of dimers formed under various conditions (see Results and Discussion below).

We used the acetone-photosensitized reaction of Ura to provide the products required for identification of the various Ura CBDs; evidence has been previously presented indicating that all four dimers are formed in this system (27). A volume of 500 mL of Ura (2 mM) was photolyzed in 167 mL batches in 80/20 water/acetone under flowing nitrogen for 45 min, as described in Supporting Information for the analogous reaction of DMU. The reaction mixture was rotatory evaporated to dryness and the resulting precipitate was resuspended in 5 mL of water. After sonication, the solution was filtered and the precipitate was set aside. The supernatant was chromatographed in 1 mL portions on Column A using the following water/methanol gradient running at 5 mL min^{-1}: 0 min, 0%; 3 min, 0%; 4 min, 12%, 5.5 min, 12%; 9.5 min, 20%; 12.5 min, 20%, 12.8 min, 0%; 17 min, 0%. Six fractions were collected, corresponding to the major peaks in the chromatogram; these are denoted as A1–A6. Fraction A1 eluted between 3.2 and 3.8 min, A2 between 4.0 and 5.0 min, A3 between 5.7 and 6.2 min, A4 between 8.7 and 9.3 min, A5 between 12.5 and 13.1 min and A6 between 13.6 and 14.1 min. Fractions A1, A2 and A4 had UV absorption spectra characteristic of those expected for CBDs, while the spectrum of A3 suggested that it was a mixture of products that contained Ura as one of the components. When the absorption spectra of appropriately diluted samples of A1, A2 and A4, each contained in a 3 mL quartz cuvette, were followed as a function of irradiation time at 254 nm, the resultant spectra in each case showed gradual conversion to the spectrum of Ura. A similar study of A3 showed the amount of absorption due to Ura increased significantly with irradiation time. HPLC of the reaction mixtures, produced by irradiation of A1 and A4, indicated that the parent peak in each case was diminished in area, while the corresponding peak for Ura was greatly increased in size; no other products were noted. However, a similar study on A2 indicated that it contained at least one major component that was resistant to photoreaction. (Column E was used for this set of studies, in conjunction with 93/7 water/MeOH flowing at a rate of 2 mL min^{-1}.) The last two fractions (A5 and A6) may be

acetone adducts of Ura, one of which has been previously reported (28). Upon irradiation at 254 nm, the product in each of these fractions reverts to Ura and at least one other component (as revealed by UV spectroscopy).

To assess the stability of the products in the various fractions to heating, a portion of each fraction was placed in a screw-top tube and heated at 100°C for 15 min (or longer). In the case of A1, the sample was heated for 15, 30, 45, 60 and 75 min; after each 15 min period of heating the solution was chilled on ice and a sample was withdrawn. HPLC of each sample was then run on Column A, using 93/7 water/methanol flowing at a rate of 5 mL min^{-1}. Under these conditions, the parent dimer(s) eluted after 2.9 min and Ura at 4.1 min. The area corresponding to the dimer decreased with heating, while the amount of Ura in the sample correspondingly increased. Between 60 and 75 min, however, relatively little change in the peak areas for Ura and dimer occurred; around 50% of the original peak area corresponding to dimer was lost after 75 min of heating. These results suggest that A1 contains two dimers, one of which is stable to heating and the second of which is unstable to reversion to Ura. Analogous heating of A4 (elution time: 7.1 min) did not lead to noticeable decomposition of the component dimer, while boiling of A2 (elution time: 3.5 min) for 15 min led to production of a small amount of Ura and sharpening of the parent peak, as compared with the unheated sample; these results for A2, along with those from study of the effect of irradiation with 254 nm light (see above) suggest that A2 contains at least two components.

To determine which of the above fractions contained the various CBDs of interest, we methylated samples of A1, A2, A3 and A4, using a procedure similar to that described above for the DMU dimers. In each case, the residue from a 1 mL portion of the concentrated fraction of interest was contained in a Sarstedt 1.5 mL screw-top microcentrifuge tube. To each residue was added the methylation reagents as described above for methylation of the DMU dimers; the resultant slurries were agitated for 16 h at room temperature. After work up, the resultant aqueous solutions of methylated reaction products were analyzed as described for the analogous reaction mixtures obtained from methylation of the DMU CBDs. Analysis of the reaction mixture obtained from methylation of A1 using Gradient D (see above) indicated that the predominant peaks had elution times of about 5.8 and 7.5 min. In separate runs, coinjection of authentic *c,s* and *c,a* DMU CBDs with the methylated sample resulted in increased areas for these two peaks and confirmed that these two peaks corresponded to the *c,s* and *c,a* DMU dimers. Additional peaks eluting at 8.2, 8.9 and 9.3 min, corresponding to the elution times for the *c,s* DMU-DMT CBD, the *c,a* DMU-DMT CBD and the *c,a* DMT dimer (see Table 1), provided confirmatory evidence that A1 was a mixture of the *c,s* and *c,a* CBDs of Ura (**Ia** and **Ib**).

Similar analysis of methylated A3 produced peaks at 5.1 and 9.1 min. Coinjection of DMU lead to enhancement of the 5.1 min peak, while coinjection of the *t,a* DMU cyclobutane dimer led to increased peak area for the 9.1 min peak. In addition, a peak eluting at 9.9 min can be assigned as the *t,a* DMU-DMT dimer, which supports the conclusion that A3 is a mixture of Ura and the *t,a* cyclobutane dimer (**Id**) of Ura. HPLC analysis of methylated A4 indicated that the predominant product eluted at 8.8 min. Coinjection with authentic, *t,s* DMU CBD led to a single peak eluting at 8.7 min with enhanced area, while coinjection with authentic *t,a* DMU dimer produced a chromatogram with two peaks, one eluting at 8.8 min and the other at 9.1 min. Thus, it can be concluded that A4 contains the *t,s* CBD of Ura (**Ic**). It is interesting to note that the elution order of the *t,s* and *t,a* Ura CBDs is reversed from that observed for the corresponding DMU dimers.

When the reaction mixture from methylation of A2 was analyzed by HPLC, nine peaks (three major and six minor) appeared in the chromatogram. It appears that this fraction is a mixture of several products, none of which is a Ura cyclobutane dimer. We made no attempt to further characterize the components of A2.

HPLC conditions for separation of the Ura c,s *and* c,a *CBDs from one another and for separating the* t,a *cyclobutane dimer from Ura*. In order to efficiently identify each of the Ura cyclobutane dimer components in various reaction mixtures and to be able to obtain a quantitative measure of the amount of each CBD produced under various photochemical reaction conditions, it is desirable to have HPLC protocols that would be effective in providing this information for underivatized reaction mixtures. (It should be noted that the methylation protocols described above were not designed for quantitative application.) While we were unable to find a single HPLC column that permitted separation of all four isomers in one run, we did develop methods that allowed us to separate the peaks corresponding to Ura and the (*c,s* + *c,a*), *t,a* and *t,s* CBDs in one run and the peaks associated with Ura and the (*t,a* + *t,s*), *c,a* and *c,s* dimers in a second run. One set of conditions utilized Column C, a Microsorb Phenyl column, with water flowing at 1.6 mL min^{-1} being the eluent. The second separation protocol used Column D, a Microsorb Amino column using acetonitrile–water mixtures as eluents. While 95%/5% acetonitrile/water flowing at a rate of 3 mL min^{-1} was most often used for elution, the eluent composition was varied between 90%/10% and 96%/4% CH_3CN/H_2O, as required in individual circumstances. As an example of the types of separations achieved, the chromatograms in Fig. 2 were obtained when the reaction mixture from the acetone-photosensitized reaction of Ura (2 mM, 20% acetone in aqueous solution, 45 min photolysis under N_2, 99% of Ura reacted) was injected on these two columns; on column D, the eluent was 95/5 CH_3CN/H_2O at a flow rate of 3 mL min^{-1}. (In general, before injection, a few mL of the solution was rotatory evaporated to dryness and, immediately after the last visible moisture had disappeared, redissolved in the same volume of water as that of the original sample. For acetone sensitization experiments, where redissolution of insoluble dimers is a problem, the protocol was slightly different; see Results and Discussion.) After spin filtration, the redissolved sample was injected directly on Column C; prior to injection on Column D, a portion of the redissolved sample was diluted 10-fold with acetonitrile. As can be seen in Panel B, the Microsorb Amino column possesses the capability of separating the *t,a* and *t,s* dimers in this particular system, as well as the *c,a* and *c,s* isomers. However, when the concentration of Ura in the injected photoreaction mixture is high, the quality of the separation on this column is significantly diminished; reliable quantitative measurements of peak areas for the *t,a* and *t,s* peaks are then difficult to obtain.

Heating of samples containing the various dimers in boiling water, followed by HPLC analysis of the resulting solutions using the same conditions, led to disappearance of those peaks in Fig. 2 corresponding to the *c,a* and *t,a* CBDs and increases in the area corresponding to Ura; corresponding decreases in the areas of peaks assigned solely to *c,s* and *t,s* dimers were not observed. This thermal behavior correlates with similar behavior observed by Jennings *et al.* (27) after they subjected the *c,a* and *t,a* CBDs of Ura to heating at 100°C. These observations support the peak assignments made in Fig. 2.

The results of the experimental work described in the sections immediately above provide the tools needed to identify the CBDs formed and to quantitatively analyze the amounts of each CBD present in photoreaction mixtures formed by irradiation of Ura under a variety of conditions. The results obtained from such qualitative and quantitative analysis of CBD content for a number of different systems will be described in Results and Discussion. The results from these analyses are useful in resolving a number of disagreements concerning product identification and quantitation that are present in the literature on Ura photochemistry.

Preparation of the (6-4) adduct of thymine. For several experiments in which the behavior of the thymine (6-4) adduct (5-hydroxy-6-4′-(5′-methylpyrimidin-2′-one)-5,6-dihydrothymine (**V**) [29]), was compared with that of the uracil (6-4) adducts, we required an authentic sample of this compound. This compound was prepared as described in Supporting Information.

RESULTS AND DISCUSSION

Here we will deal with two main topics. The first is establishment of the structures of those water-soluble photoproducts formed when Ura is irradiated in the frozen state at dry ice temperature. The second is identification of the Ura CBDs and provision of relative quantitative measures of the amounts of these CBDs formed when Ura is irradiated under a variety of conditions.

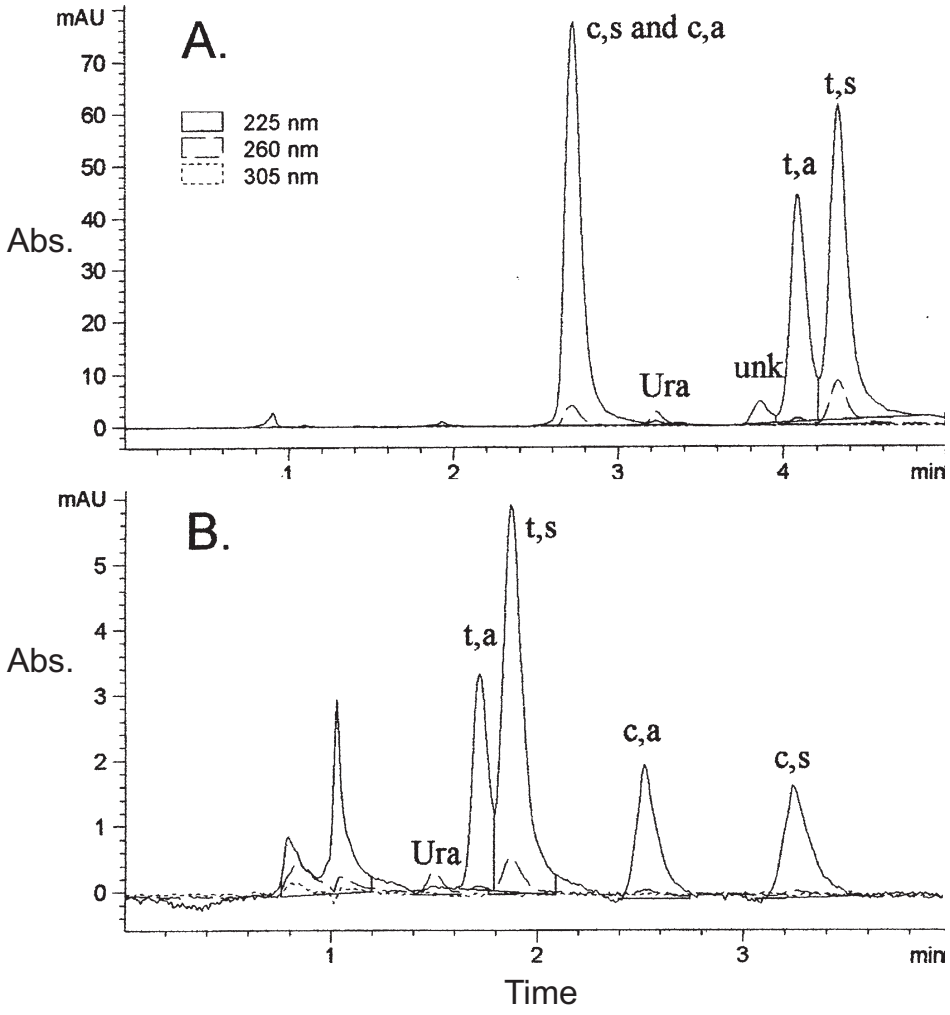

Figure 2. The HPLC chromatograms resulting from injection of the mixture resulting from acetone-photosensitized reaction of uracil (2 mM) on a Microsorb Phenyl column (panel A) and a Microsorb Amino column (panel B). Preliminary sample preparation and elution conditions are described in Materials and Methods. The traces at three different wavelengths are overlapped in each chromatogram.

Photochemistry in the aqueous Ura system in the frozen state: Purification of (6-4) adducts from F2 and F3 and a hydrated form of a uracil trimer from F1

In the following paragraphs, we describe the isolation and characterization of the two (6-4) adducts and a trimer hydrate of uracil. The work described below uses as a starting point the fractions F1, F2 and F3 that were isolated during the first-pass fractionation of the photoreaction mixture resulting from irradiation of aqueous Ura in the frozen state, as described in Materials and Methods.

Typical protocols for purification of the products contained in F1, F2 and F3. Fraction F2 contained the major putative (6-4) adduct, termed P2, along with significant amounts of cyclobutane dimer impurity. While difficult to remove using a Capcell UG120 column, an excellent separation of P2 from dimer was achieved using a phenyl column (Column C). After rotatory evaporation of F2 to dryness and redissolution in 2 mL of doubly distilled water, the resultant solution was rechromatographed, using 200 μL injections with doubly distilled water (1.6 mL min^{-1}) as eluent. P2 eluted after 2.4 min, while residual dimer came off after 2.7 min. The resulting P2 was repurified using the same conditions.

The minor putative (6-4) adduct, P3, contained in F3, was rechromatographed on a Column D using 85/15 acetonitrile/water flowing at 4 mL min^{-1} as eluent. Before chromatography, F3 was taken to dryness by rotatory evaporation and redissolved in 1 mL of 80/20 acetonitrile/water. Then 100 μL injections of F3 were made on Column D; the desired compound eluted at 2.5 min, while various impurities eluted after the main peak. The predominant impurity, eluting at 3.0 min, was the uracil photohydrate **II** (9), identified by comparison of its properties with those of an authentic sample.

To accomplish the separation of the components of F1, 100 μL portions of concentrated F1 were diluted with 200 μL of acetonitrile and the resulting 300 μL samples were chromatographed on Column D using 70/30 acetonitrile/water flowing at 3 mL min^{-1}. Two main peaks, eluting at 1.2 min (F1-1) and 1.8 min (F1-2), were collected. Irradiation of F1-1 at 254 nm yielded only Ura as a product, indicating that F1 was contaminated by cyclobutane dimer. Upon analytical

HPLC of the reaction mixture after irradiation of F1-2 at 254 nm, using Column D, both Ura and a peak with the same elution time as P2 (see above) came off the column; some **IV** was present as well. Only very small amounts of F1-2 could be isolated.

Determination of the nature of the photoproducts P1-2, P2 and P3. We used UV spectroscopy, mass spectrometry and chemical studies to establish the nature of P1-2 and, in addition, used NMR spectroscopy to study P2 and P3.

The available evidence suggests that P1-2 is an adduct of a trimeric form of Ura with water. Because of the very small amounts of this product that were isolated, we were unable to establish the detailed structure of this compound; however, two lines of evidence support the description of this compound as being trimeric in nature. As mentioned above, photolysis of P1-2 at 254 nm yields two main products; these were identified by HPLC as being Ura and a compound having the properties of P2 (which is shown to be a (6-4) adduct in the next paragraph). This is similar to the behavior observed when the water adduct of the thymine trimer is similarly irradiated (30). The ESI mass spectrum of P1-2, run in the positive ion mode, shows peaks at 377.26 and 393.34 corresponding to the sodium and potassium adducts of a compound with the molecular formula $C_{12}H_8N_6O_7$, the chemical formula of a trimer of uracil to which has been added a molecule of water. A weak peak corresponding to the protonated form of the parent trimer hydrate is also present, as is a peak corresponding to the protonated form of the trimer itself. Early mass spectral evidence, indicating a polymeric compound with a molecular mass of 370 is formed when Ura is irradiated in the frozen state at dry ice temperature, was obtained by Khattak and Wang (20); they suggested that this compound was a trimeric species. As the observed molecular mass of this compound differs significantly from the value obtained here and, as it is indicated that the putative trimer reverts to uracil upon irradiation (20) and is extremely labile (see Wang [19], p. 334), the relationship of the putative trimer of Khattak and Wang to the one described here is unclear. Indeed, Jennings *et al*. (27) suggested, based on IR studies, that the substance identified as a trimer by Khattak and Wang contained a mixture of the *c,s* and *c,a* dimers of Ura (see below for further discussion).

The purified products P2 and P3 were each subjected to study by mass spectrometry, NMR spectroscopy and UV spectroscopy. The high resolution ESI mass spectrum of P2 was obtained on a Brucker Fourier Transform 9.4 T instrument in the positive ion mode. This spectrum yielded a molecular mass of 225.06451, which corresponds to a protonated species containing two uracils with a molecular formula of $C_8H_9N_4O_4$. Interestingly, we were unsuccessful in obtaining a molecular mass of P2 using MALDI mass spectrometry, possibly due to facile decomposition of the adduct in the acidic matrix. However, MALDI-MS of P3, using α-cyano-4-hydroxycinnamic acid as a matrix, yielded a parent ion peak with a mass of 225.060 based on internal calibration, again corresponding to the molecular mass expected for a protonated dimeric form of uracil.

Proton NMR data are consistent with both P2 and P3 being (6-4) adducts, with one having the structure shown as **IIIa** and the other with the structure indicated by **IIIb**. The relevant chemical shift and splitting constants are given in Table 2. All of the expected protons are present. The resonances for the C5 and C6 protons of P3 are very close in chemical shift; the resulting two proton multiplet spectrum is quite complex, complicated by coupling of C6H with NH1. Upon addition of a small amount of D_2O, this multiplet was transformed into a quartet, which could be analyzed as an AB spectrum, as described by Becker (31), p. 136. The chemical shifts of the C5 and C6 protons for both P2 and P3 are consistent with those expected for protons located in a saturated uracil ring, while those of the C5′ and C6′ are similarly consistent with expectation for protons located at in an unsaturated uracil ring.

The presence of three exchangeable protons in the spectra obtained for P2 and for P3, as shown by the disappearance of the resonances for these protons after addition of small amounts of D_2O to the NMR samples contained in d_6-DMSO, is also in agreement with predictions from the proposed structures **IIIa** and **IIIb**. In the case of P2, we were able to measure the coupling constant for the interaction of C6H with N1H as being 3 Hz. We also obtained a ^{13}C NMR spectrum for P2. The chemical shift data are shown in Table S1, along with the corresponding ^{13}C data that we obtained for **V**. (While this latter (6-4) adduct has been extensively studied {see

Table 2. Proton NMR data for the (6-4) adducts of uracil.

(6-4) adduct	C5′H	C6′H	C5H	C6H	N1H	N3H	N1′H
IIIa (d_6-DMSO)	6.27 (d, 6.6)	7.87 (broadened)	4.45 (d, 6.8)	4.51 (dd, 6.8,3)	7.72 (broadened)	11.9 (v. broad)	10.1 (broadened)
IIIa (D_2O)	6.71 (d, 6.2)	8.07 (d, 6.2)	4.85 (d, 6.9)	4.95 (d, 6.9)			
IIIb (d_6-DMSO)	6.41 (d, 6.0)	7.99 (d, 6.0)	4.23 (complex multiplet)	4.23 (complex multiplet)	7.88	11.9 (broadened)	10.2 (broadened)
IIIb (d_6-DMSO + D_2O)	6.42 (d, 6.0)	7.99 (d, 6.0)	4.230 (d, 6.6) or 4.253 (d, 6.6)*	4.230 (d, 6.6) or 4.253 (d, 6.6)*			

Proton NMR spectra were run at 600 MHz on a Varian INOVA NMR spectrometer. TMS was used as an internal standard in DMSO, while TSP was used for this purpose in D_2O. Each of the peaks gave an appropriate integration area for the number of protons expected. Coupling constants in Hz are given in parentheses after the chemical shifts of the corresponding CH proton in ppm. In general, the resonances observed for protons attached to nitrogen in both **IIIa** and **IIIb** in DMSO-d_6 either disappeared or became greatly diminished in peak area after addition of small amounts of D_2O. The connectivity of C5′H and C6′H in **IIIb** was verified *via* a COSY experiment.

*Upon addition of D_2O, to the d_6-DMSO solution of **IIIb**, the broadened quartet-like multiplet centered at $\delta = 4.23$ simplified to a distinct quartet centered near $\delta = 4.24$, reflecting loss of coupling of C6H to the exchangeable N1H proton. The δ values given for C5 and C6 were calculated using standard methods for analysis of AB spectra; it is not possible to assign either of these two resonances to a specific proton.

[19] for leading references}, the ^{13}C NMR spectral data for **V** has not been previously published.) As can be seen, the chemical shifts for the corresponding carbons in the two structures are reasonably close to one another; this provides additional support for the assignment of P2 as a (6-4) adduct.

All of the above spectroscopic data are consistent with the assignment of the structures of P2 and P3 as (6-4) adducts, as described by structures **IIIa** and **IIIb**. However, chemical studies also provide strong supporting evidence for these structural assignments. Boiling an aqueous 0.1 M HCl solution of each of these compounds for 5 min results in its conversion to compound **IV**; this product differs from **IIIa** and **IIIb** in that it has lost the elements of a water molecule from positions C5 and C6. (Dehydration of P2 and P3 is much slower in boiling water in the absence of acid.) The structure of **IV** has been previously established by Khattak and Wang (20), based on UV, NMR and mass spectral evidence. This result rules out an alternative possibility, namely that either P2 or, alternatively, P3 is a (5-4) adduct, similar to that shown in **VI**. Dehydration of **VI** would lead to a compound with the structure shown by **VII**. However, the UV spectrum of **VII** is available in the literature (32); comparison of the UV spectrum of **VII** (Fig. 5 in Bergstrom and Leonard [32]) with that of **IV**, shown in Fig. 2 in Khattak and Wang (20), shows that the two spectra are very different. This disproves the hypothesis that either P2 or P3 is a (5-4) adduct.

Compound **VII** is present in small amounts in solutions arising from irradiation of 2 mM Ura on dry ice as described above. When such a solution is chromatographed using 92/8 (10 mm sodium phosphate, pH 7.6)/MeOH at 2 mL min^{-1} on Column B, a compound elutes after 3 min with an absorption maximum at 353 nm. Using a procedure similar to that of the previous workers (32), we prepared authentic **VII** by irradiating 10 mL of a deoxygenated solution containing 2 mM uracil and 1 mM 4-thiouracil in a 20 mL Pyrex tube with black ray lamps (Spectronics BLE-1800B) for 1 h. In agreement with expectation from the results of the previous work, HPLC of the resulting solution on Column B, using 92/8 (10 mm sodium phosphate, pH 7.6)/MeOH at 2 mL min^{-1}, showed that two main products were present, namely compounds with absorption spectra similar to those provided by Bergstrom and Leonard (32) for **VII** and 5-4′-(pyrimidin-2′-one)-4-thiouracil. The first of the compounds eluted at 2.9 min and had an absorption spectrum identical to that of the corresponding peak arising from HPLC of the irradiated uracil solution. The second eluted at 5.0 min and had an absorption spectrum similar to that given previously for 5-4′-(pyrimidin-2′-one)-4-thiouracil (32). As expected, the compounds assigned as **VII** coeluted when the irradiated Ura and 4-thiouracil-Ura solutions were coinjected. As observed by Bergstrom and Leonard (32), **VII** has a low solubility in aqueous solution and precipitates when irradiated solutions are concentrated.

The exact profile of the spectrum of **VII** with respect to wavelength is sensitive to the pH of the eluting solvent. In our initial runs, using doubly distilled water as the aqueous component of the eluting solvent, we found that there was some variability from run to run of the diode array spectra corresponding to putative **VII**; consequently, it was difficult to establish with certainty that the spectrum of the putative **VII** formed in the uracil solution irradiated on dry ice was identical to that produced *via* irradiation of 4-thiouracil with Ura. However, when the pH was fixed by use of 10 mM phosphate buffer (pH 7.6) as the aqueous component of the eluent, then the absorption spectral profiles became identical.

Solutions of Ura, freshly irradiated on dry ice and then thawed, are always slightly yellow-green in color. However, none of the compounds discussed above have absorption tails extending into the visible region. We therefore carefully examined the absorption spectrum of freshly irradiated 2 mM uracil solutions in the visible region and found evidence for a weak absorption band with a maximum around 427 nm. Upon allowing unconcentrated solutions to stand in the cold for several weeks, some cyclobutane dimer precipitates; however, this dimer precipitate has a yellowish cast, suggesting that this compound (hereafter termed Z) has a limited solubility. Concentration of freshly irradiated solution by rotatory evaporation leads to precipitation of uracil CBD on the sides of the flask holding the solution. While there is an increase in absorbance of the supernatant at $\lambda = 427$ nm as concentration proceeds, a substantial portion of Z appears to be lost by coprecipitiation with uracil cyclobutane dimer. We were unable to isolate enough of Z for characterization. However, we were able to characterize its HPLC retention properties and obtain its absorption spectrum using the spectral capture capability of the diode array detector. Using 92/8 (10 mm sodium phosphate, pH 7.6)/MeOH at 2 mL min^{-1} on Column B, Z elutes at 1.4 min; using these same elution conditions, uracil elutes at 0.95 min, **VII** elutes at 3.0 min and a composite peak corresponding to cyclobutane dimer and (6-4) adducts elutes at 0.85 min. In addition to a broad maximum in the spectrum of Z at 427 nm, there are two shallow minima at 287 and 345 nm between which lies a second maximum at 320 nm. Approximate ratios of the absorbances, obtained using the diode array detector, have the following values: $A_{427}/A_{320} = 4.9$; $A_{427}/A_{287} = 5.9$; $A_{427}/A_{345} = 5.8$.

An effort was made to obtain a rough estimate of the relative amounts of combined (6-4) adduct (**IIIa** + **IIIb**) and **VII**. To do this, we measured the absorbances of a freshly irradiated Ura solution (2 mM) at 304, 357 and 427 nm. After subtraction of spectral background at the wavelengths of interest, the residual absorbance of a freshly irradiated solution of 2 mM Ura at 304 nm is 0.207, the absorbance at 353 nm is 0.037 and the absorbance at 427 nm is 0.017. From the measured spectrum of Z, the ratio of the absorbance at 353 to that at 427 nm is $A_{353}/A_{427} = 0.54$, while the corresponding value of A_{304}/A_{427} is about 0.20. Using these ratios, we can calculate the contribution of the absorbance of Z to the measured absorbance values at 304 and 357 nm and correct these two values to those that would be measured at these wavelengths in the absence of Z. The corrected values are 0.028 at 354 nm and 0.204 at 304 nm. As the (6-4) adducts have negligible absorbance at 353 nm, we can use an estimated value of 22 900 (based on an average of the values for ε_{max} given by Bergstrom and Leonard [32] of 23 500 at pH = 2 and 22 300 at pH 10) to estimate a value of 1.2 μM for the concentration of **VII**. From the published absorption spectrum (Fig. 5 in Bergstrom and Leonard [32]), it can be estimated that the ε value of **VII** at 304 nm is about 7900. Using the calculated concentration of **VII**, the contribution of **VII** to the absorbance of the solution at 304 nm can be evaluated as 0.0096. Thus, the value of the combined absorbance at 304 nm due to **IIIa** and **IIIb** can be evaluated as being about 0.190.

Using an estimated value of ε_{max} = 4900 at 304 nm (that of the thymine 6-4 adduct) and assuming as an approximation that **IIIa** and **IIIb** have the same ε value, we calculate the concentration ([**IIIa**] + [**IIIb**] to be 38.9 μM. Thus, it can be estimated that the concentration of 6-4 adduct is about 32-fold greater than that of **VII**. Assuming that all **VI** produced (**VI** being the putative precursor of **VII**) indeed decomposes to **VII**, then this calculation suggests that production of (6-4) adducts is a considerably more facile reaction that that leading to (5-4) adduct when frozen aqueous solutions of uracil are irradiated on dry ice.

Suggestive evidence that P2 and P3 have the structures IIIa and IIIb, respectively. The spectroscopic and chemical evidence presented above strongly supports the hypothesis that both P2 and P3 are (6-4) adducts of uracil. However, this evidence does not provide a definitive indication as to which product has the structure given by **IIIa** (in which the hydroxyl group and the 2′-pyrimidone ring are *cis* with respect to one another in their attachment to the dihydropyrimidine ring) and which corresponds to **IIIb** (in which the OH group and the 2′-pyrimidone ring are *trans* with respect to each other). Indeed, definitive assignment of the structures must await X-ray diffraction studies, such as was done in the assignment of the conformation of the corresponding known thymine (6-4) adduct (**V**) to a structural type analogous to **IIIa** (33). One could reason from analogy that P2 corresponds to **IIIa**, based on the fact that it is the predominant form produced in the photoreaction and that this is the only form that, thus far, has been reported to form when thymine is irradiated under similar conditions at dry ice temperature. However, there are experimental observations that, combined with quantum mechanical calculations, strongly support the hypothesis that P2 has the structure **IIIa** and, therefore, that P3 can be assigned the structure **IIIb**. Our initial observation was that when purified P2 is chromatographed on Column D (a Microsorb Amino column packed with silica particles to which aminopropyl groups are bonded) using 85% acetonitrile/15% water as eluent, a significant fraction of the injected parent material is lost. In its place, a significant sized broad peak elutes with UV spectral properties identical to those of **IV**. A plausible reason for this instability of P2 is that interaction of this molecule with free amine groups, associated with the column packing, in some manner induces loss of water in the C5-C6 region of the dihydropyrimidine portion of the molecule. An analogous reaction is not observed when P3 is chromatographed. Indeed the injected P3 can be quantitatively recovered. Thus, the amino column appears to induce selective elimination of water from P2, as compared with P3. (It was for this reason that a Microsorb Phenyl column was used to purify P2, but a Microsorb Amino column could be used for final purification of P3.)

A generalized description of the above reaction is elimination of a molecule HX from a parent molecule to form a double bond. While a number of types of mechanism have been proposed to explain such elimination reactions, the so-called E2 mechanism is usually invoked to explain conformation-selective behavior of the type described above. (For a detailed discussion of elimination reactions, see Chapter 17 in Smith and March [34]; the E2 mechanism is discussed on pp. 1478–1486.) Other types of elimination mechanism are not generally regarded as displaying such a high degree of selectivity. Explanation of the selective elimination of water from P2, as compared with P3, by invoking an E2 mechanism requires that P2 be able to adopt a conformation that is not accessible to the P3 molecule (see below). Viewing the amino column-induced reaction in this context, an unprotonated alkyl amine, bound to the silica column packing, would act as a catalytic attacking base, removing hydrogen from C6H, and the hydroxyl group at C5 would depart simultaneously with the hydrogen at C6. This is shown schematically in Fig. 3, in which departure of hydroxyl is assisted by the availability of protonated amine. For this mechanism to be feasible, a fraction of amino groups must exist in the unprotonated state within the Microsorb Amino column. While the pK_a of propylamine is 10.57 ([35], p. 163), Varian (the column manufacturer) indicates that the pK_a of the NH_2 packing is 9.8 (Varian Catalog of Chromatography and Spectroscopy Products and Accessories, 2003–2004, p. 9). The actual percentage of amino groups present as free amine within the column packing is difficult to assess, as it probably depends on the history of the column. Our column has been used mainly with eluents that were mixtures of acetonitrile and double distilled water (generally degassed under vacuum, filtered and stored under air in sealed Pyrex bottles until used), although it has also been used with 25 mM ammonium formate as the aqueous component of the eluent. In view of the unknowns concerning the state of amino groups within the column packing, it is probably not fruitful to draw conclusions about the mechanism of dehydration of P2, based solely on the observation that this reaction occurs during passage through the Mircrosorb Amino column. Instead, we carried out experiments with another aliphatic amine in solution, namely methylamine (MeA), to determine if P2 was again selectively dehydrated, as compared with P3. The theoretical basis for believing such selective dehydration might occur for P2, assuming it is indeed **IIIa**, is given immediately below. This development is followed by a discussion of our experimental results.

As indicated above, if an E2 mechanism is invoked to explain the selective dehydration of P2 (with accompanying identification of this compound as **IIIa)**, as compared with P3 (which then would be identified as **IIIb)**, an important stereochemical question must be answered; this question deals with the range of conformations available to **IIIa**, as compared with **IIIb**. Facile E2 mechanisms require that the hydrogen removed by base be able to take an *anti*-periplanar orientation

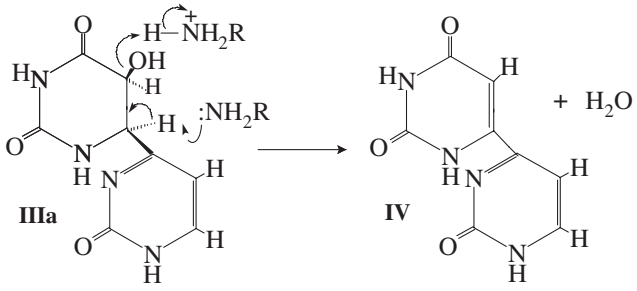

Figure 3. Depiction of the E2 mechanism as a pathway for the decomposition of the product P2 (putatively **IIIa**) to **IV**, as induced by aminopropyl groups associated with the packing of Microsorb Amino columns and by aqueous 500 mM methylamine at pH 10.1. Discussion is given in the text.

with respect to the leaving group (the hydroxyl group). Thus, if P2 is to be identified as **IIIa**, then it must be shown that the species **IIIa** can take up an *anti*-periplanar conformation and that **IIIb** does not have access to this same conformation. Considering torsional strain induced by the groups attached to C5 and C6 bonds in the dihydropyrimidine moiety of **IIIa**, could such an *anti*-periplanar conformation indeed be accessible to **IIIa** and not available in **IIIb**? To answer to this question, we used Spartan '08 for the Macintosh to calculate the torsional energy profile of **IIIa** as a function of the dihedral angle between the C5O and C6H bond of the dihydropyrimidine ring in **IIIa**. These calculations were done using the Hartree-Fock model with a 3-21G basis set and the protocol detailed in the Tutorial and Users Guide for Spartan '08 ([36], pp. 98–101). (The dihedral angle in this situation is defined as the angle between two planes, both passing through the length of the bond between C5 and C6, with one plane passing through the C5O and the other through the C6H bond. An angle of −180° [or 180°] corresponds to the conformation where the C5O bond and the C6H bond are *anti*-periplanar, while a value of 0° [or −360°] describes the case where these two groups are periplanar.) The energy profile generated by the set of calculations is displayed in Fig. 4. These results for **IIIa** indicate there are two energy minima, one near −180° (the *anti*-periplanar conformation) and a significantly deeper one at about −65°. Thus, the calculations indicate that the *anti*-periplanar conformation of **IIIa** is not only accessible, but is located at a torsional energy minimum. Similar calculations performed on **IIIb** indicate that the deepest minimum in the torsional energy is at about −55°, that there is a shallow minimum at 55° and that the torsional energy is very high in the *anti*-periplanar conformation at 180° (see Fig. 4). The periplanar conformation at 0° is available for **IIIb**, although at an energy that is elevated above the corresponding energy curve minimum. While *syn*-elimination can occur from periplanar conformations *via* the E2 mechanism, it is usually considerably less facile then *anti*-elimination and occurs only when the *anti*-periplanar conformation cannot be achieved (Smith and March [34], p. 1482). As it is unlikely that **IIIb** can take up an *anti*-periplanar conformation under any conditions, it would be expected to be considerably less labile than **IIIa** towards elimination of water *via* an E2 mechanism in the presence of bases, such as aliphatic amines. Assuming an E2 mechanism is indeed operative, observation of facile elimination for P2 and absence of elimination (or considerably slower elimination) would strongly suggest that P2, the major (6-4) adduct, is **IIIa** and P3 is **IIIb**.

It should be noted that the quantum chemical results calculated *via* Spartan, including the minima in the potential energy curve displayed in Fig. 4, correspond to the situation predicted in vacuum at 0 K; the relative energies of the various conformations of **IIIa** in solution (*e.g.* in the aqueous MeA reaction system) or when interacting with the aminopropyl column packing could have significantly different values than those calculated. However, because steric factors forbid a molecule with structure **IIIb** from taking up an *anti*-periplanar structure, conclusions about the unlikelihood of a species with this structure undergoing reaction *via* an E2 mechanism should be unaltered in these situations.

As indicated above, we carried out exploratory experiments, in which we examined the question of whether methylamine

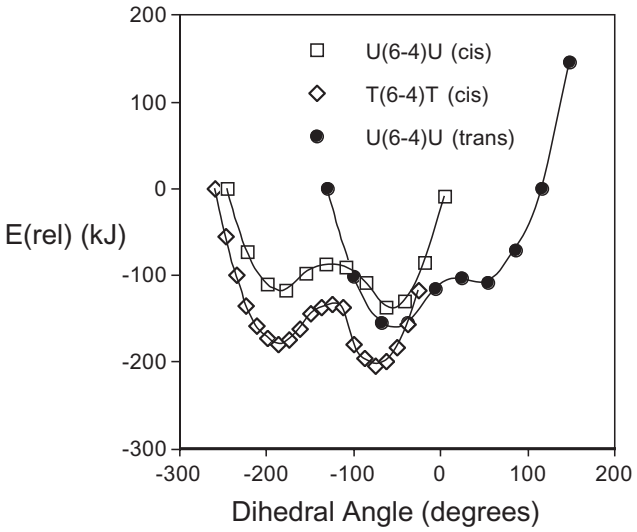

Figure 4. The potential (torsional) energies of **IIIa**, **IIIb** and **V**, displayed as a function of the dihedral (torsional) angle about the bond between C5 and C6 in the dihydropyrimidine partner in these adducts. The dihedral angle in this situation is defined as the angle between two planes, both passing through the length of the bond between C5 and C6, with one plane passing through the C5O and the other through the C6H bond. An angle of −180° (or 180°) corresponds to the conformation where the C5O bond and the C6H bond are *anti*-periplanar, while a value of 0° (or −360°) describes the case where these two groups are periplanar. These three potential energy curves was generated using Spartan '08 for the Macintosh to calculate the torsional energy profile of the three molecules as a function of the dihedral angle between the C5O and C6H bond of the dihydropyrimidine ring portions of **IIIa**, **IIIb** and **V**. These calculations were done using the Hartree-Fock model with the 3-21G basis set and the protocol detailed in the Tutorial and Users Guide for Spartan '08 ([36], pp. 98–101). In general, these calculations are initiated by constraining the relevant dihedral angle to a particular initial value and then seeking the equilibrium geometry of the molecule under this constraint; the relevant output for the purpose of the graph is the total energy of the molecule when in this equilibrium geometry. The constraint is then changed by a user selected angle increment and a new equilibrium geometry and its corresponding energy are evaluated. This is repeated until a user selected final value of the dihedral angle is reached. The relative energies appearing on the graph are those calculated by subtracting the calculated total energy of the initial conformation from the total energies of various constrained conformations for which calculations were done. Care was taken to select initial and final dihedral angles, such that Spartan was able to carry out all calculations without providing an "error" message at any stage of the sequence of calculations; such signals usually signify the presence of unacceptable steric overlaps. The body of the paper contains detailed discussion of the implications of the information contained in this figure.

(MeA), (pK_a = 10.62 [35]), can induce selective dehydration. An initial study was made, in which P2 and P3 were adjusted to the same absorbance (0.92) before making a 1/1 dilution with 1 M MeA (pH 10.1). Injections of 20 μL samples, taken after varying times of incubation at 19°C, were made on Column B using 90%(10 mM sodium phosphate buffer, pH 7.6)/10% MeOH flowing at 2 mL min^{-1} as eluent; the temperature was controlled during the reaction by placing the aqueous incubation medium in a Dewar flask. Attention was focused on material eluting at about 1.6 min, corresponding to **IV**. The striking end result of this experiment was that over a 48 min time interval in which P2 was incubated, the measured peak area for **IV** (at 304 nm) increased from an

undetectable level to 90 area units; the corresponding measured area of **IV** in the incubation of P3 increased from 2 to 5 area units. A control experiment was carried out using the same conditions, in which P2 was incubated in 0.1 mM NaOH; the pH of the 0.2 mM parent solution was adjusted, so after two-fold dilution its pH was 10.1. After 36 min incubation, the amount of **IV** detected at 304 nm increased from 0 to 8 area units. This result indicates that MeA is responsible for most of the dehydration occurring at pH 10.1, rather than hydroxide anion coming from reaction of MeA with water.

It should be noted that **IV** elutes as a pair of broad overlapping peaks, the major peak eluting at 1.51 min and the minor peak at 1.71 min, both peaks having identical absorption spectra; the ratio of peak areas, measured at 304 nm, was about 8/1. No other peaks were doubled. The same behavior was noted in experiments made with Column C, described below; however, with the phenyl column, the corresponding ratio of peak areas was about 3/2. The reason for this chromatographic behavior of **IV** appears to be associated with incomplete neutralization of MeA in the injected sample by the 10 mM phosphate buffer used as eluent (see below). When **IV**, prepared by heating of P2 with 0.1 M HCl for 10 min, followed by rotatory evaporation to dryness and dissolution in distilled water, was injected on the phenyl column using 95%(10 mM sodium phosphate buffer, pH 7.6)/5% MeOH flowing at 1.6 mL min^{-1} as eluent, a single sharp peak eluted. When a sample of this material was diluted two-fold with 1 M MeA, pH 10.1, and injected, two overlapping broader peaks resulted; the material in these two peaks had identical absorption spectra. In this paper, the sums of the two peak areas corresponding to **IV** were used for analyses requiring such data.

The results described above, taken in aggregate, suggest that selective dehydration of P2, as compared with P3, can indeed be induced by alkyl amines. However, Column B was unable to optimally separate certain MeA associated impurity peaks, eluting near the retention times of P2 and P3**,** from these two compounds; thus, we elected to use another column to do studies on the kinetics of disappearance of these two compounds. For this purpose, we used Column C (a Microsorb Phenyl column), which led to excellent resolution of P2 and P3 from impurities and reaction products. In experiments with P2, we incubated 140 μL samples of this compound (contained in 1.5 mL plastic snap-top tubes) in 500 mM MeA (pH = 10.1) for varying lengths of time at 19°C. In a representative experiment, the sample for incubation was prepared by diluting 70 μL of aqueous parent adduct solution (OD_{304} = 3.36) with 70 μL of 1 M MeA (pH 10.1), followed by vortexing and then starting the timer. The concentration of amine can be regarded as constant during the course of the reaction and, therefore, the second order kinetics predicted by the E2 mechanism can be simplified to pseudo first order kinetics. After withdrawal and injection of an initial sample of 10 μL after 0.5 min of incubation, succeeding samples of 10 μL were taken after appropriate intervals (spaced in the neighborhood of 12 min) over a 64 min time period and subjected to analytical HPLC on Column C; the eluent was 95%(10 mM sodium phosphate buffer, pH 7.6)/5% MeOH flowing at 2 mL min^{-1}. Using these elution conditions, P2 eluted at about 1.8 min and the dehydration product **IV** eluted at 3.6 min. The areas of the peaks corresponding to P2 and **IV** were measured, using detection at 304 nm. In our analysis, we used the fact that, in 1st order kinetics, quantities proportional to concentration can be used in lieu of concentrations themselves to determine rate parameters. We found that the rate of disappearance of peak area corresponding to the parent compound obeyed 1st order kinetics; the value of the rate constant for disappearance of P2, calculated from the slope of a linear plot (ρ = 0.992) of the natural log of the area corresponding to [P2] *vs* time, was 0.014 min^{-1}. When the peak areas corresponding to **IV** were plotted as a function of time, the resultant graph had the shape expected for a product produced by a 1st order reaction ($Area_{IV} = [Area_{IV}]_0$ {1−exp[−kt]}). These experiments were conducted two more times, using a different elution condition (97%[10 mM sodium phosphate buffer, pH 7.6]/3% MeOH flowing at 1.6 mL min^{-1}). In both runs, the first order plots were linear (ρ > 0.99) and the values of the two calculated rate constants for disappearance of P2 were both calculated to be 0.014 min^{-1}.

Analogous studies were done with P3; in these experiments, it was found that the parent compound was relatively stable. In a typical experiment, we diluted 200 μL of P3 (OD_{304} = 0.30) with 200 μL of MeA (1 M, pH 10.1) and incubated as above for a total of 58 min. The reaction mixture was sampled five times over the 58 min time interval and the withdrawn samples (50 μL) were analyzed using HPLC on Column C (95%[10 mM sodium phosphate buffer, pH 7.6]/5% MeOH flowing at 2 mL min^{-1}). Plotting the natural log of the peak area, measured at 304 nm, as a function of time yielded a straight line (ρ = 0.999); the rate constant for disappearance of P3 was calculated from the slope to be 0.003 min^{-1}. However, only barely detectable amounts of **IV** were formed during this time interval. The production of traces of **IV** could be interpreted as being due to P3 undergoing a slow *syn*-elimination process; however, we cannot rule out the possibility that this **IV** is formed from residual P2 impurity remaining in P3, even after careful purification. Repetition of the same experiment with P3 several times, as outlined above, led to similar results each time.

We did one further set of experiments to determine if the rate of reaction does indeed depend on amine concentration. When incubation of P2 was done in 100 and 250 mM MeA, both at pH 10.0 and 19.0°C, and the resultant solutions were analyzed as above on Column C after appropriate time intervals, the pseudo first order rate constants for disappearance of P2 were evaluated to be 0.006 and 0.010 min^{-1}, respectively. These results do indicate a dependence of the rate of reaction on amine concentration dependence; however, rather than the expected ratio of 2.5 for the rate constant in 250 mM solution (in a pure E2 mechanism), compared with that in 100 mM solution, the observed ratio is 1.67. The corresponding ratio for the rate constants obtained for 500 mM (pH 10.1) and 250 mM are 1.50, instead of 2.

The results of the experiments on P2 and P3 described in the above paragraphs are remarkable, in that they give a clear-cut indication that dehydration to form **IV** in 500 mM MeA solution at pH 10.1 is highly selective for P2, as compared with P3. The results of the quantum chemical calculations, described above, also indicate **IIIa** should be much more susceptible to facile dehydration by an E2 mechanism than **IIIb**. Thus, assuming an E2 elimination mechanism (or E2-like

mechanism; see below) is operative, the dehydration behavior of P2, compared with P3, is consistent with the identification of P2 as **IIIa** and P3 as **IIIb**. We have assumed this is the correct assignment in labeling the NMR data given in Table 2 and Table S1 and in the discussion that follows below. These results also lend credence to the idea that the observed selective dehydration of P2 (**IIIa**) on the amino column is due to interactions with the free amino groups contained within the column packing.

Our results provide a starting point for further detailed studies of the mechanism of dehydration of P2. It must be considered that the mechanism may, in fact, not be pure E2, but instead may lie close to E2 in the "E1-E2-E1cB spectrum", as discussed by Smith and March (34) (p. 1494); this is important due to the fact that OH is a poor leaving group and in view of our preliminary evidence suggesting that the dependence of the rate of the dehydration reaction is nonlinear in unprotonated amine concentration. Results from further experiments (*e.g.* studies of the dependence of the kinetics on amine concentration and on pH; studies with other amines having different pK_a values; studies of kinetic isotope effects) will be required to draw more definitive conclusions about the mechanistic pathway for dehydration of **IIIa** induced by amines.

Upon first consideration, it might be thought that the thymine (6-4) adduct (**V**), being analogous to **IIIa**, should be similarly unstable towards decomposition upon the Microsorb Amino column. Calculations for **V** using the same protocol, employing the Hartree-Fock model and 3-21G basis set used in the calculations for **IIIa**, indicate that there are minima in the torsional energy profile at about the same values of the dihedral angle as for **IIIa** (see Fig. 4). Thus, the results of these calculations suggest that **V** can take indeed up the *anti*-periplanar conformation that is desirable for facile elimination *via* an E2 mechanism. Experiment, however, shows that **V** is stable to HPLC on this column. In addition, we found **V** to be stable when incubated in MeA solution (500 mM, pH 10.1, 19°C) under the same conditions where **IIIa** underwent facile elimination of water. If the E2 mechanism is to be given weight as a possible mechanism for amine-induced decomposition of **IIIa**, then there must be a reason for stability of **V** under the same conditions. A possible explanation can be found in the greater accessibility of the C6 hydrogen to free amine groups on the column (or in MeA solutions) in the case of **IIIa**, as compared with the accessibility of the corresponding hydrogen in **V**. Examination of the structures of **IIIa** and **V**, both in the *anti*-periplanar conformation, indicates that the two methyl groups present in **V**, but not in **IIIa**, offer a degree of protection of the C6 hydrogen from interaction with free amine groups in the column packing or in solution. Similar protection of C6H is not evident in the corresponding structure for **IIIa**. (These two structures, shown side-by-side in Figure S1 in color, were generated as side products of the torsional energy calculations described above.)

Plausible mechanistic pathways describing formation of the (6-4) isomers **IIIa** *and* **IIIb**. It is thought that CBDs and the (6-4) adducts (or the putative oxetane [or azetidine] precursors [19]) of the pyrimidine nucleobases and related compounds in the frozen state are produced within microcrystallites of these compounds; these microcrystallites are formed as a result of exclusion of nucleobase from water during the freezing process. (For a review of the physical processes that occur in the freezing of aqueous solutions, including formation of solute aggregates, and the chemistry and photochemistry that can occur in the aggregates contained in such frozen solutions, see Montenay-Garestier *et al.* [37].) It appears that thermal reactions of primary oxetane photoproducts can result in their conversion to secondary products upon warming of frozen solutions containing photolyzed aggregates. For example, Rahn and Hosszu (38) have studied the conversion of putative oxetane precursor, produced by irradiation of Thy in ice at −196°C, to Thy(6-4)Thy as a function of temperature and concluded that, upon annealing the frozen irradiated solution for 10–20 min at various temperatures, this conversion process could occur at temperatures as low as −80°C. The rate of conversion increased with increasing temperature between −80 and 0°C. As irradiations on dry ice occur at about −78.5°C, it is likely that conversion of oxetane precursor to Thy(6-4)Thy adduct occurs continuously throughout the period that frozen solutions containing Thy are irradiated at this temperature. One possible interpretation of these results is that as the temperature of annealing is increased, shells containing increasing amounts of mobile interfacial water are formed around the Thy microcrystallites containing the oxetanes; such mobile water would then be available to catalyze the conversion of precursor oxetane to Thy(6-4)Thy. Another possibility is that water trapped within microcrystallites might become increasingly available for reaction as temperature increases. While we have not conducted similar studies of temperature dependence of conversion of putative oxetane precursor to Ura(6-4)Ura in irradiated frozen solutions of Ura, it seems reasonable that the same type of behavior could be expected in this system as well. It is interesting to note that Ura photohydrate **II** (6-hydroxy-5,6-dihydrouracil [9]) was found as a minor product in the photoreaction of Ura in dry ice (see the discussion concerning the purification of P3 above). This suggests that mobile water may be available to photoexcited uracils within microcrystallite lattices at this temperature.

Figure 5 displays a plausible reaction scheme *via* which compounds with structures **IIIa** and **IIIb** could be formed from a common oxetane intermediate. In this figure, two Ura molecules react photochemically to form an intermediate oxetane (Int-1). (A more realistic visualization of the structural framework of Int-1, albeit as the optical isomer, is shown in Fig. 6; for sake of clarity, all hydrogens have been removed except those at C5 and C6 on the dihydropyrimidine ring.) This intermediate can react with the oxygen of an incoming nucleophile (*e.g.* water) in two ways. A nucleophilic backside attack (relative to the oxetane oxygen [labeled Ox] at the carbon labeled 4′ in Fig. 6) would lead to breaking of the oxetane ring bond to the 2-pyrimidone ring; loss of a proton from the added water and protonation of the oxygen formerly associated with the oxetane would lead to Int 2a (Fig. 5), in which the *cis* stereochemical configuration of this oxygen, relative to the 2-pyrimidone ring, is retained. Loss of water from the 2-pyrimidone ring would then lead to formation of **IIIa**. Alternatively, nucleophilic backside attack (again relative to the oxetane oxygen) by a water molecule on the carbon labeled 5 in the dihydropyrimidine ring of Int-1 (see Figs. 5 and 6) would eventually lead to **IIIb**. The resultant

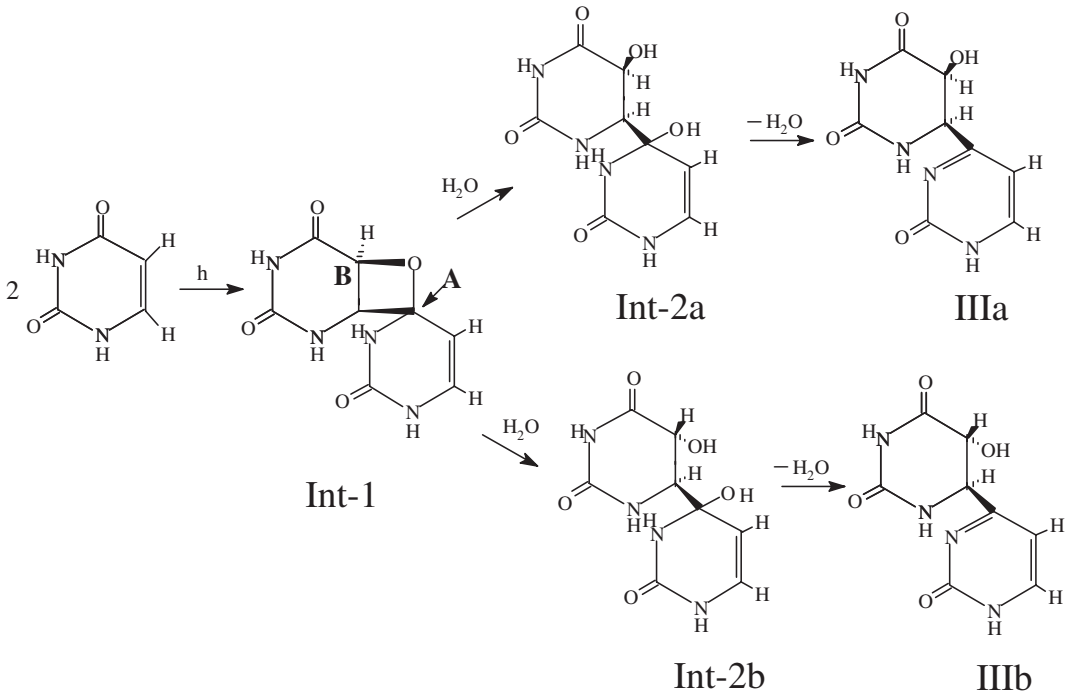

Figure 5. Reaction pathways leading to formation of **IIIa** and **IIIb** from the common oxetane intermediate Int-1, as discussed in the text. A more realistic rendering of the structure of Int-1 in its alternative enantiomeric form is given in Fig. 6.

displacement of the oxygen of the oxetane ring would lead it to becoming associated with the pyrimidone ring. The incoming oxygen from the water, after deprotonation to form a hydroxyl group, would have a stereochemical configuration in which it is *trans* to the 2-pyrimidone ring. Loss of water from the pyrimidone ring then leads to **IIIb**.

Another possibility to consider is that species, other than water, capable of inducing oxetanes to undergoing ring-opening reactions could be concentrated in a mobile water shell surrounding microcrystallites containing oxetanes, or, alternatively, contained as contaminants within the microcrystallites. (In this regard, it is interesting to note that irradiation of frozen solutions containing a 2/1 mixture of Ura/Thy at dry ice temperature resulted in the formation of the Thy(6-4)Ura adduct [39], indicating that microcrystallites formed upon freezing do not necessarily contain a single species.) Such contaminant species might be hydrogen or hydroxide ions and their counterions. For example, hydrogen ion could protonate O4′ of the oxetane; this could be followed by N3′-lone pair assisted conversion of this protonated species to **IIIa**. Alternatively, OH^- could act as a nucleophile in a manner similar to the mechanism illustrated above with water. Concentration of such species, along with their counterions, would occur because the freezing process in water excludes solutes (such as Thy or Ura) and impurities. Solute and impurity molecules would be concentrated into smaller and smaller volumes as freezing of the parent solution proceeded to completion; presumably volumes of water containing solutes and impurities would be the last to freeze (40). Kinetic and other studies of frozen aqueous nucleobase systems, to which deliberate additions of varying amounts of acidic or basic species (*e.g.* HCl or ammonia) have been made, might yield insights leading to definitive elucidation of the processes occurring in the conversion of oxetane to two forms of (6-4) adduct.

There are no reports in the literature indicating that the *trans* configuration of the Thy(6-4)Thy adduct has been isolated and characterized. It is therefore interesting to ask the question "Why does not thymine photoreact to form a similar *trans* form of the Thy(6-4)Thy adduct?" This question can be addressed by comparing the relative accessibility of C5 in Int-1, the oxetane precursor to Ura(6-4)Ura, to that of C5 in the thymine analog of Int-1 (see Fig. 5). Quantum mechanical calculations of the equilibrium conformations of these two compounds yielded the structures shown in color in Figures S2 and S3, these figures show both ball and tube and space filling models of these two compounds. (Details of the calculations, carried out using Spartan 08, are given in the caption of Fig. 6.) Examination of Figure S2 indicates that access to the C-5 carbon in the Ura version of Int-1 is very open, while corresponding access to C-5 in the thymine oxetane intermediate is highly restricted, due to blockage by the 5-methyl group on the dihydropyrimidine ring. However, when the 4′-carbon is examined, access to water is equivalent in the two structures (see Figure S3). This suggests that the enhanced reactivity of Ura towards formation of the *trans* form of Ura(6-4)Ura, as compared with reactivity to produce the corresponding Thy product, is due to steric blockage of access of water to C5 in the latter case.

It is interesting to note that the C5 position in the putative oxetane or azetidine precursors to Cyt(6-4)Thy and Cyt(6-4)Cyt adducts would be predicted to be more accessible to nucleophilic attack than C5 in the Thy(6-4)Thy adduct. It is thus possible that both forms of these two adducts would be formed under suitable UV-irradiation conditions, perhaps

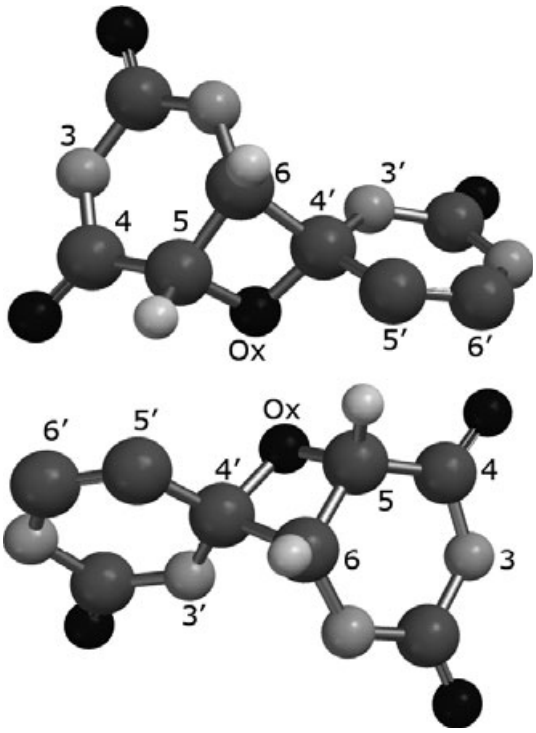

Figure 6. Two views of a ball-and-stick model of the 4′R,5S,6S isomer of the putative oxetane precursor of the (6-4) adduct of uracil. This is the enantiomer of Int-1 displayed in Fig. 5. All hydrogens, except those located at C5 and C6, are hidden. Oxygen atoms are denoted by black balls, nitrogens by light gray balls and carbon atoms are coded by medium gray. The oxygen of primary interest is labeled Ox. As described in the text, backside attack of water at C4′ in line with the C4′-Ox bond would lead to **IIIa** and analogous attack at C5 would produce **IIIb**. This model was constructed using Spartan '08 for the Macintosh to calculate the equilibrium ground state conformation. The sequence of calculations used was as follows. A set of conformers was sought *via* molecular mechanics calculations using the MMFF force field. Only one low energy conformer was found. The equilibrium geometry of this conformer was determined using semiempirical calculations utilizing the PM3 model. The equilibrium conformation determined in this round of calculation was then reoptimized using the Hartree-Fock model with the 3-21G basis set. The equilibrium conformation was then given a final optimization using the Hartree-Fock model and the 6-31G* basis set. Informative alternative views of this compound are displayed in color in Figures S2 and S3.

even in a biological context. Similarly, one might expect two forms of the Ura(6-4)Thy and Ura(6-4)Cyt adduct could be prepared under appropriate conditions.

Identification and measurement of the relative yields of the cyclobutane dimers of Ura formed under various irradiation conditions

In Materials and Methods, we discussed the results of studies of the HPLC behavior of the Ura CBDs. We indicated that through use of two columns, namely a Microsorb Phenyl column (Column C) and a Microsorb Amino column (Column D), separations can be obtained such that the peak corresponding to each dimer is reasonably well resolved from the peaks corresponding to the other components of a reaction mixture containing all of the dimers and Ura. In this section, we apply this methodology to identifying the dimers produced and the relative yields (based on peak area) in which they are formed for a number of photoreaction systems.

Identification and determination of the relative yields of the dimers formed when uracil is irradiated in frozen solution. In the early 1960s, a number of workers noted that irradiation of Ura in the frozen state at dry ice temperature yields product(s) that were shown to have the character of CBDs (40–43). However, there was not uniform agreement among these researchers concerning the number and properties of the dimers formed in this photochemical reaction. For example, Wacker and coworkers (42) indicated that one isomer was formed, while Smith (43) found that two products appeared after paper chromatography, one with an R_f of 0.12 and the other with an R_f of 0.01. Smith noted that the faster moving material converted into the slower moving material upon standing, while the slower moving compound could be reconverted to the faster moving dimer by treatment with acid, alkali or heat. (Demonstration that two crystalline forms of the *c,s* Ura dimer exist was accomplished by Varghese [21] and independently by Jennings *et al*. [27]; one form is much less soluble than the other. Insoluble dimer spotted at the origin probably accounts for the $R_f = 0.01$ spot.) The findings of Smith and of Wacker *et al*. diverged somewhat in another way, as the latter workers found that the dimer they observed was unstable to boiling in water for 15 min and to treatment with acid or base. Smith, in agreement with results from Smietanowska and Shugar (41), found that the dimeric material he studied was stable under similar conditions. Later work also contained suggestive evidence that more than one dimer was formed. For example, Blackburn and Davies (44) found that initially isolated dimer was partially degraded by treatment with formic acid, leaving a residual amount of undecomposed material identical to the starting material. After methylation of the "ice dimer" of Ura, Elad *et al*. (24) noted that the end product was contaminated with the *c,a* dimer of DMU. Varghese (21) indicated, in his study of the photoreaction of Ura in the frozen state, that about 10% of the dimer formed was the *c,a* isomer, the remainder being the *c,s* form. Structural identification of the *c,s* dimer has been carried out using chemical studies in conjunction with NMR spectrometry (44), by X-ray diffraction study (45) and by chemical degradation studies (46). The structure of the *c,a* isomer has been derived from a X-ray diffraction study. This crystalline dimer, obtained after irradiation of Ura in the frozen state, was obtained by crystallization of the *c,a* cyclobutane dimer from the product mixture resulting from boiling a sample containing a putative uracil trimer (47); this *c,a* form of the dimer was thought to be a trimer decomposition product. (See, however, Jennings *et al*. [27], p. 489, where an alternative interpretation of the crystallization of the *c,a* cyclobutane dimer from solutions containing the putative trimer is given.)

When we analyzed the photoreaction solution, resulting from irradiation of aqueous Ura (2 mM) in the frozen state for 1 h, using the two-column approach described towards the end of Materials and Methods, it was found that, in fact, all four CBDs are formed. Peak area measurements for the HPLC chromatogram, obtained using the Microsorb Phenyl column, showed that 90% of the total integrated area at 225 nm for CBD peaks was found under the (*c,s* + *c,a*) peak, while 6.5%

was under the *t,a* peak and 3.5% was under the *t,s* peak. When the same reaction mixture was run on the Microsorb Amino column, the *c,s* peak and *c,a* peaks contained 63% and 37%, respectively, of the total area under these two peaks. Therefore, it can be calculated that the distribution of areas for the four peaks corresponding to cyclobutane dimer is 57% *c,s*/33% *c,a*/3.5% *t,s*/6.5% *t,a*. (In general, the percentages listed here, as well as in the following paragraphs, are based on average peak areas calculated from integrated peak area values for several runs.) These results indicate that the fraction of *c,a* dimer formed is somewhat higher than previously estimated by Varghese (21), who used ion exchange chromatography to separate the two isomers. The formation of the two *trans* isomers when Ura is irradiated in the frozen state has not been previously reported. (It should be emphasized that the relative yields we present for the various CBDs may differ from those that would be obtained *via* methods that directly yield measures of molar concentrations of these products. To convert our results to this type of measure, we would need to know ε values for the various CBDs at 225 nm; such information is not presently available for these compounds.)

Identification and distribution of the yields of dimers formed when photoreaction of Ura is sensitized by acetone in fluid aqueous solution. Krauch *et al*. (48) and Greenstock and Johns (49) published early indications that all four CBDs of Ura are formed when acetone is used to photosensitize the reaction of the parent compound in aqueous solution. Based on experiments in deoxygenated solution (unspecified concentration of Ura) using radiotracer techniques, Greenstock and Johns found that the various isomers were produced in comparable amounts and provided quantitative measurements of the amount of each dimer formed, while Krauch *et al*. identified one of the dimers as the *c,s* form. The chemical identities of the dimers corresponding to each measured yield were not established by Greenstock and Johns; however, data from experiments done by the same workers with Ura in frozen solution permits identification and quantitation of the relative amounts of the *c,s* and *c,a* isomers formed. From their data, it can be calculated that the ratio of yields of *c,s* CBD to *c,a* CBD is about 60/40. Later work by Varghese (21), employing 50% acetone and Ura at a concentration of 2 mM, measured the amounts of dimer found in each of two phases. After 125-fold concentration of the original photolyzed solution, the precipitate formed was filtered off and the yields of the various CBDs in the supernatant were found to be 68% *c,s*/29% *c,a*/0% *t,s*/3% *t,a*. Infrared spectroscopic examination of the precipitate, after washing with methanol to remove Ura, indicated to Varghese that it contained the *t,a* dimer as the predominant product. Based on calculations that took into account the weight of the precipitate, he concluded that the *t,a* dimer was the major form of CBD produced in the acetone-sensitized photoreaction of Ura. In work published at about the same time, Jennings and coworkers (27) presented their findings on the acetone-sensitized reactions of Ura. While they did not evaluate quantitative yields of the various dimers, they did identify those dimers that dominated after irradiation of 10 mM Ura in water/acetone mixtures of compositions ranging from 5% to 83% V/V acetone/water. In agreement with Varghese, the supernatant was found to contain predominately the *c,s* and *c,a* forms of the dimer, as well as some *t,a* CBD. These workers also found that a precipitate formed during irradiation for each acetone-sensitized reaction they studied. Their analysis of each individual precipitate implied that it consisted of predominately *t,s* dimer with some *t,a* CBD contamination; only the *t,s* form remained after the precipitate was treated with boiling water. They also found that at least one component of the precipitate was unstable to treatment with ammonia; about 13% of the weight of the precipitate was converted to Ura, the product that they determined was formed by treatment of the *t,a* dimer with ammonium hydroxide. Thus, there is significant conflict between the results of Varghese and those of Jennings *et al*. concerning the nature of the dimers making up precipitates resulting from the photoreaction of Ura using acetone-sensitization.

New experimental results suggest that the Ura t,s CBD is produced in greater amounts than the t,a CBD in acetone sensitized reactions. To help resolve the disagreement between the results of Varghese and those of Jennings *et al*., we conducted two studies; one looked at the composition of the freshly prepared reaction mixture resulting from acetone-sensitized reaction of Ura and then examined the composition of the same mixture after a precipitate had been allowed to form. The second study determined the composition of the precipitate formed when the acetone-sensitized reaction was run as described by Varghese in his study. Specifically, our first study was designed to determine the ratios of yields of the various dimers formed when the photoreaction of Ura (2 mM) was sensitized by acetone (20% V/V). About 175 mL of solution was irradiated for 45 min under flowing 99.997% nitrogen that bubbled through the solution. (Prior to flowing into the reaction vessel, the nitrogen was bubbled through a solution that was of the same composition as the reaction medium.) We then analyzed the dimer content of this solution immediately after irradiation and after standing overnight at room temperature. (After standing, a significant amount of precipitate could be observed in the flask containing the irradiated solution.) Samples (0.5 mL) of the freshly reacted solution were placed in Sarstedt screw-top microcentrifuge tubes and most of the acetone was removed by rotatory evaporation on a water aspirator, as described in Materials and Methods. The remaining solution was rediluted to 0.5 mL, injected successively on the Microsorb Phenyl and Microsorb Amino columns and analysis of the resulting chromatograms was carried out as described above. The following area ratios were obtained for the various dimers: 19% *c,s*/18% *c,a*/39% *t,s*/24% *t,a*. The corresponding ratios for the solution that had stood overnight were: 29% *c,s*/27% *c,a*/20% *t,s*/24% *t,a*. It can be seen that a considerable loss of the *t,s* CBD from the parent solution occurred on standing, along with a smaller loss of the *t,a* dimer. (If loss of *t,a* CBD had not occurred from solution upon standing, the percentage of this dimer in solution would have been higher than 24%, rather than remaining constant at this value.) These results imply that the precipitate formed upon standing contains both the *t,s* and the *t,a* Ura CBDs. (In experiments with freshly irradiated solutions, care must be taken that precipitation does not start before or during sample workup. Otherwise, there can be significant variation from the results described above. This variability is likely due to partial precipitation of the relatively insoluble *trans* dimers prior to injection; this particularly true

of the *t,s* CBD. Such precipitation causes the calculated amounts of the *trans* dimers to be lowered, as compared with the *cis* dimers.)

In the second study, we irradiated 2 mM Ura in 50% acetone under nitrogen and worked up the resulting photoreaction mixture as described by Varghese (21). The resulting precipitate, after washing with methanol, was dried in air. We then methylated a weighed amount of this precipitate with CH_3I in a slurry containing Ag_2O in DMF as described in Materials and Methods. After workup as described previously, the HPLC of the methylated sample was run using the same column and gradient as previously described. While quantitative assessments cannot be made, the resulting chromatogram showed strong peaks corresponding to both the *t,s* and *t,a* DMU-DMU dimers. Also present was a peak eluting at the retention time of the *t,s* DMU-DMT dimer and a peak corresponding to the overlapping retention times of the *t,s* DMT dimer and *t,a* DMU-DMT CBD (see Table 1). There was not any evidence for the presence of methylated *c,s* or *c,a* CBDs of Ura in the sample. In a second experiment, the precipitate was heated for 1 h in boiling water, the resulting mixture was taken to dryness and the resultant solid material was methylated as above and subjected to HPLC. Analysis of the chromatogram produced indicated that the peaks corresponding to the methylated dimers of the *t,a* isomer were greatly diminished in area, as compared to the corresponding peaks assigned as belonging solely to methylation products of the *t,s* dimer. This is agreement with expectation, as Richter and Fahr (50) remarked on the greater thermal lability of the *t,a* cyclobutane dimer of Ura, as compared to the *t,s* form. This is also in agreement with the thermal behavior of the *t,a* (and *c,a*) CBDs formed in photoreactions of thymine; the half-life of the *t,a* CBD of thymine at 100°C in neutral solution, with respect to reversion to thymine, is only a few minutes (see, *e.g.* Fig. 11 in Fisher and Johns [8]). Summarizing, our results imply that both *t,s* and *t,a* CBDs are significant components of the precipitate that was isolated using the workup methods employed by Varghese to study mixtures of Ura CBDs produced *via* sensitization with 50% acetone; our results confirm that the *c,s* and *c,a* CBDs remain in solution during precipitate formation.

The conflicting conclusions of Varghese (21) and of Jennings *et al.* (27), regarding the photochemistry occurring in acetone-sensitized solutions of Ura, have been resolved by the information obtained in our work. Our results indicate that the precipitate studied by Varghese, instead of consisting of mainly one dimeric form (the *t,a* CBD) as he proposed, was a mixture containing significant amounts of both the *t,s* and *t,a* isomers. While done in more concentrated solutions of Ura (10 mM *vs* 2 mM, as used in the experiment of Varghese and in our replication of his experiment), Jennings *et al.* also observed that the precipitates formed during irradiation contained both of the *trans* dimers. Furthermore, our determination of the composition of freshly photosensitized reaction mixtures show that the *t,s* dimer is the product present in largest amount; in the supernatant of solutions that had stood overnight, the *t,s* dimer was present in the smallest amount, while some *t,a* dimer had also been lost. This lost material must have ended up in the precipitates that were formed upon standing. All of these observations strongly support the conclusion that precipitates formed in acetone-sensitized reactions contain a mixture of both *trans* dimers as indicated by Jennings and co-workers.

Based on the above discussion, along with careful consideration of the protocols and results of the two previous workers, some retrospective suggestions can be made about reasons why Varghese and Jennings *et al.* differed in some of their conclusions. Both Varghese (21) and Jennings *et al.* (27) used IR spectroscopy as their prime tool for identification of the dimer(s) present in the precipitates resulting from their photoreactions. Jennings and co-workers published IR spectra for each of the dimers they obtained. They indicated that the identity of the isomer corresponding to each spectrum was verified by comparisons with IR spectra provided to them by Professor E. Fahr, in whose laboratory authentic samples of each of the four dimers had been prepared *via* nonphotochemical synthetic methods (50,51). Varghese similarly published four IR spectra that he designated as being for the α and β forms of the *c,s* dimer, the *c,a* dimer and the *t,a* cyclobutane dimer of Ura and indicated that the latter dimer had been synthesized using the procedure of Richter and Fahr (50); the IR spectrum of the *t,s* CBD was not included in the paper. However, comparison of the IR spectra given in the two papers indicates that the spectrum that Jennings *et al.* (27) identify as being that of the *t,s* isomer is labeled as being the *t,a* isomer by Varghese (21). Varghese indicates that his conclusion that the precipitate was composed mainly of *t,a* cyclobutane dimer was based on comparison of the IR spectrum of the precipitate he obtained, after irradiation of 2 mM Ura in the presence of 50% acetone, with the IR of the compound that he identified as the *t,a* isomer. Thus, in contrast to the identification made by Jennings and coworkers, Varghese concluded that the precipitate was made up mainly of *t,a* CBD. This juncture of disagreement led to other disagreements in interpretation. Varghese indicated that column chromatography of the substances contained in the precipitate, using 0.1 N ammonia as eluent, resulted in destruction of about 90% of the chromatographed material and suggested that the product produced was a cyclobutane dicarboxylic acid. In contrast, Jennings and co-workers, after studying the stability of the compound they identified as the *t,a* CBD to treatment with concentrated ammonia, concluded that the reaction product was uracil. They found that similar treatment of the compound they identified as the *t,s* dimer produced an unidentified compound with an IR band at 1400 cm^{-1}. (It can be noted that the carboxylate ion functional group has a symmetric stretching mode vibration at 1400 cm^{-1} (see, *e.g.* Pasto and Johnson [52], p. 127)). In another experiment, Varghese found that heating his putative *t,a* CBD at 100°C for 15 min had no effect (see Table 1 in Varghese [21]). In contrast, Jennings and co-workers found that refluxing of the dimer they identified as *t,a* in boiling water for 24 h resulted in conversion of this compound to uracil, while the *t,s* isomer were stable to this treatment. The agreement of this behavior with the previously reported analogous thermal properties for these two dimers (50) was used by Jennings *et al.* to confirm the identifications of the *t,a* and *t,s* isomers based on IR spectra.

Identification and distribution of the yields of dimers formed when uracil is irradiated in fluid aqueous solution. The photoreactions of Ura in fluid aqueous solution have received a

significant amount of study, although much of this attention has been focused on the reaction to form the hydrate of Ura (see the discussion in Fisher and Johns [9]). However, there is also published information concerning the formation of CBDs. Greenstock *et al*. (53) indicated that irradiation in fluid aqueous solution produced several dimers, while Brown and Johns (54) found that all four dimers were produced. Using radiotracer techniques, Greenstock and Johns (49) measured the relative yields of the four dimers when Ura was directly irradiated in deaerated aqueous solution at an unspecified concentration. As the yields of the *c,s* and *c,a* dimers can be determined (based on identification of these two compounds from a study of reactions of Ura in the frozen state reported in the same paper), the ratio of the amounts of these two isomers can be evaluated as 54/46. Relevant data from other sources is also available. Unpublished work by Varghese (cited in Fisher and Johns [8], p. 244) indicated that the ratio of dimer product yields was 35% *c,s*/15% *c,a*/0% *t,s*/50% *t,a* (irradiation done at an unspecified Ura concentration) while Fendler and Bogan (55), using radiolabeled Ura and paper chromatography to study the photochemistry of Ura at a concentration of 10^{-4} M in degassed aqueous solution, found this ratio to be 15% *c,s*/78% *c,a*/3.5% *t,s*/3.5% *t,a* after DMU, in an actinometric solution irradiated in parallel, had been converted to products to an extent of 77.1%. Presence of oxygen in the solution of Ura strongly suppressed formation of CBDs. (It should be noted that product distribution in uracil systems directly irradiated in solution with 254 nm light is potentially sensitive to the percent conversion of parent to product as well as initial concentration; as the percentage conversion of parent uracil to product increases, dimeric products become increasingly able to compete with the parent for light with consequent CBD photoreversal. As a competing photoirreversible hydration reaction occurs in the case of Ura, the amounts of the total and individual cyclobutane dimer products present in solution may increase and then decrease with increasing reaction time; indeed, such behavior is observed in the data presented in Table 1 of the paper by Fendler and Bogan.)

We examined the dimer distribution in two different situations where Ura was irradiated at 254 nm in fluid solution under flowing nitrogen. In the first, we irradiated 170 mL of 2 mM Ura for 3 h as described in Materials and Methods; about 41% of parent Ura had reacted. Analysis of the results from HPLC, as described above, indicated that in this system the area ratios for the dimer distribution was 20% *c,s*/26% *c,a*/22% *t,s*/32% *t,a*. In the second experiment, we irradiated 170 mL of deoxygenated 10^{-4} M Ura concurrently with 170 mL of 10^{-4} DMU at 254 nm; the two solutions were placed in equivalent positions in the lamp holder described in Materials and Methods and irradiated for 12 min. After this time, 78.6% of the DMU had disappeared, which is close to that obtained in the experiment of Fendler and Bogan cited above (77.1% DMU conversion). In this situation, the corresponding area ratio was found to be 15% *c,s*/24% *c,a*/26% *t,s*/35% *t,a*.

The ratio of *c,s*/*c,a* of 44/56 calculated for the direct reaction of 2 mM Ura is in reasonable agreement with the value of 56/44 evaluated from the data of Greenstock and Johns (49) (see above), particularly taking into account that different methods of quantitation were employed and that considerably different concentrations of Ura may have been used for the two sets of experiments. Consideration of the arguments given in the discussion of the experiments of Varghese (21) on the acetone-sensitized photoreaction of Ura (see above) suggests that the value of 50% *t,a* CBD measured in his unpublished work may, in fact, reflect contributions from both the *t,s* and *t,a* forms of the cyclobutane dimer.

There is considerable discrepancy between the results of Fendler and Bogan and the results published here for the situation when a 10^{-4} M solution of Ura is irradiated in fluid solution. Fisher and Johns (8) (p. 249) suggested that the disagreement in observed product ratios, between the work of Varghese (done at unspecified concentration) and that of Fendler and Bogan, could be due to three possible reasons: mistaken identification of the dimers, to the effects of concentration on the product ratios or to changes in dimer ratios with increasing time of irradiation. Comparison of results from the present work (15% *c,s*/24% *c,a*/26% *t,s*/35% *t,a*) in which about 79% of the DMU in an actinometric solution had been converted to product, to those published by Fendler and Bogan (15% *c,s*/78% *c,a*/3.5% *t,s*/3.5% *t,a*) in which 77% of the DMU in a similar solution was converted to product suggests that the latter two reasons can be ruled out as causes for major changes in product ratios and that misidentification of photoproducts is a more plausible explanation. It is worth noting that failure to resolve the *c,a*, *t,s* and *t,a* dimers, with accompanying identification of the composite paper chromatography spot as the *c,a* CBD, would lead to an artificially high apparent *c,s*/*c,a* ratio of 15/85. Similar addition of the area contributions of the *c,a*, *t,s* and *t,a* dimers observed in our work, to obtain the area of a composite spot, would give an analogous *c,s*/*c,a* ratio of 15/85. Under these circumstances, the products identified by Fendler and Bogan as *t,s* and *t,a* dimers would be minor noncyclobutane dimer photoproducts. In support of the idea that other unidentified products are produced when 10^{-4} M Ura is irradiated in aqueous solution, our solutions contained an unidentified product that, upon HPLC using Column C with distilled water as eluent, eluted between the peak for Ura and the peak corresponding to *t,a* dimer; the absorption spectrum corresponding to this peak was similar to those observed for the *c,s*, *c,a* and *t,a* CBDs of Ura. (The uracil hydrate elutes before Ura under these elution conditions.) The percentage contribution of the area for this peak (monitored at 225 nm) to the total area observed for all product peaks (excluding the hydrate of Ura) was about 6%; this can be compared with the value of 7% observed for the sum of the contributions of the putative *t,a* and *t,s* dimers to the total dimer yield, as evaluated by Fendler and Bogan. If the scenario described here should be valid, it would help account for the discrepancy between the results of the work of Fendler and Bogan and the other results discussed above.

Identification and distribution of the yields of the dimers formed when uracil is irradiated in acetonitrile solution. There have been two studies made of the photochemistry of Ura when dissolved in acetonitrile. Both studies were designed to examine questions relevant to understanding the excited state(s) responsible for reaction and to gather kinetic data describing the various excited state processes that Ura undergoes when photolyzed in acetonitrile. The work of Lamola and Mittal (56) in 0.7 mM solution indicted that two dimers were

Table 3. Distribution of the yields* of individual Ura cyclobutane dimers.

Uracil System	% *c,s*	% *c,a*	% *t,s*	% *t,a*
2 mM, frozen in dry ice†	57	33	3.5	6.5
2 mM, acetone photosensitized, freshly irradiated	19	18	39	24
2 mM, acetone photosensitized, stood overnight	29	27	20	24
2 mM, fluid aqueous solution	20	26	22	32
0.1 mM, fluid aqueous solution	15	24	26	35
0.17 mM in acetonitrile, 75% conversion to product	18	18	32	32
0.17 mM in acetonitrile, 17% conversion to product	14	14	52	20

*Yields were evaluated using HPLC peak areas as described in the text of the paper; these numerical values represent averages from several runs. Peaks were detected at 225 nm.
†Solution was not deoxygenated. All other systems were flushed with 99.997% pure nitrogen prior to irradiation.

formed, while the work of Wagner and Bucheck (57) in 0.19 mM solution suggested that all four isomers might be formed, based on analogy with results from the work of Krauch *et al*. (48) on the photosensitized reaction of Ura in aqueous solution.

Using the protocols described above, we identified the dimers formed and measured the peaks areas corresponding to each dimer using a concentration of Ura approximating one of those employed by Wagner and Bucheck. We prepared a stock saturated solution of Ura in acetonitrile by stirring 56 mg of Ura overnight in 500 mL of HPLC grade CH_3CN. Making the assumption that the ε_{max} for Ura in CH_3CN is about the same as that in water, we determined that the concentration of the supernatant solution was 0.87 mM. We than diluted a portion of the concentrated supernatant to a concentration of 0.17 mM and used this solution for our experiments. A 3 mL portion of the 0.17 mM solution was placed a cylindrical irradiation tube and prepared for irradiation as described in Materials and Methods. The spectrum was measured against the acetonitrile blank (see Materials and Methods) after being irradiated for 0, 15, 30, 60, 90, 120 and 150 s. After 150 s, about 75% of the initial absorbance of Ura had disappeared. (It should be noted that the orientation of the external surface of the tube with respect to the entering light beam in the spectrometer was the same for each spectral measurement and in measurement of the blank; failure to do this resulted in severe displacements of the baseline and consequent unusable spectra.) When a similar run was done under air, the reaction was much slower, with 16 min irradiation required to achieve 66% conversion of parent Ura to product. Analysis of the product mixture resulting from irradiation under N_2, using the Microsorb Amino and Microsorb Phenyl columns as described above, showed that all four CBDs are indeed formed and that the distribution of areas for the product peaks after 150 s irradiation was 18% *c,s*/18% *c,a*/32% *t,s*/32% *t,a*. The reaction mixture obtained from 15 s irradiation (17% conversion of Ura to products) was similarly studied; the corresponding distribution was 14% *c,s*/14% *c,a*/52% *t,s*/20% *t,a*. It is interesting to note that the 15 s sample contains a relatively high content of *t,s* dimer, as compared with the 150 s sample. The probable reason for this is that the *t,s* dimer has a somewhat higher molar absorbance at 254 nm than the other three dimers (such is the case for the thymine CBDs; see Table 13, p. 277, in Fisher and Johns [8]). As a result, the *t,s* dimer is likely to be more susceptible to photoreversal at high extents of conversion than the other three dimers.

Summarizing discussion. The results of our measurements of the distribution of dimer yields, based on measurement of chromatographic peak areas, are summarized in Table 3. As a result of the studies on the CBDs produced when Ura is irradiated under various conditions, the following general conclusions can be drawn.

1. Both the *c,s* and *c,a* CBDs are formed in major amounts when Ura is irradiated in frozen aqueous solution with the *c,s* dimer being the predominant dimer (57% yield) and the *c,a* dimer being present to the extent of 33% of the total dimer product formed (based on HPLC peak areas measured at 225 nm). The *t,a* and the *t,s* dimers were produced in smaller yields, amounting in total to about 10% of the total dimer product yield. These results resolve inconsistencies in results reported in the literature, some suggesting that only one dimer was formed and others that two were produced when Ura is irradiated in ice. Our findings also address the findings of some workers that heat or acid instability was associated with the dimeric product(s) formed; one of the major products produced, the *c,s* isomer, is stable to heat and acid treatment, while the other major product (the *c,a* CBD) is unstable to similar treatment.
2. When Ura is irradiated in fluid solution (*e.g*. in water or acetonitrile) all four CBD isomers are formed in significant amounts under each of the conditions studied. This is also true when the photoreaction of Ura is sensitized by acetone. Our results, along with careful comparison of results and analysis of experimental protocols used in previous work, allowed us to make plausible suggestions about how several inconsistencies in the literature can be resolved.

CONCLUDING REMARKS

It has been shown in this study that two diasteromeric (6-4) adducts are formed when Ura is irradiated in frozen solution. This is the first report indicating that a (6-4) product can be formed, in irradiations of pyrimidine nucleobases and related compounds, with the 5-hydroxy and 6-pyrimidone groups *trans* with respect to one another A plausible mechanism is proposed, showing how two diasteromeric forms can be generated from the type of oxetane intermediate thought to be a precursor of (6-4) adducts. It has also been shown that photoreaction of aqueous Ura in the frozen state generates a trimeric species as well as a (5-4) adduct (which was detected as its dehydration product) and uracil hydrate. Also reported

here are definitive identifications of the CBDs formed in a several types of photoreaction systems containing Ura (*i.e.* in the frozen aqueous state, in fluid aqueous and acetonitrile solution and in aqueous acetone-sensitized reaction systems). Quantitative measures of the yields of the four dimers in each of these systems are also given; these measures are based on analysis of HPLC peak areas. Reports of the results of prior work on the photochemistry of Ura are incomplete in their description of the photochemistry occurring in these systems and, in some cases, in disagreement. Based on the work reported here, suggestions for resolving several contradictions in the literature have been made and a fuller picture of the photochemistry of Ura has emerged.

Acknowledgements—Research support from the National Science Foundation (CHE-0131203) is gratefully acknowledged. We thank Professor Arnold Falick and Dr. David King of the Mass Spectrometry Laboratory, Howard Hughes Medical Institute, University of California, Berkeley, CA and Michael Cohen of the Kip Guy laboratory at the University of California, San Francisco, for running mass spectra of the various adducts and Janet Chung of the Tom James laboratory at the University of California, San Francisco for running several proton NMR spectra. We also thank the two anonymous reviewers for their careful critiques and useful suggestions concerning various aspects of the original manuscript.

SUPPORTING INFORMATION

Additional Supporting Information may be found in the online version of this article:

Appendix S1. Preparation of DMU and DMT cyclobutane dimers and the (6-4) adduct of Thy

Figure S1. Ball and stick (top) and space-filling (bottom) depictions of **IIIa** and **V** in an *anti*-periplanar conformation.

Figure S2. Equivalent perspectives of the 4′R,5S,6S enantiomers of the putative oxetane precursors of the (6-4) adduct of uracil and the corresponding adduct of thymine, shown as both ball and stick (top) and space-filling models (bottom).

Figure S3. Another pair of equivalent perspectives of the 4′R,5S,6S enantiomers of the putative oxetane precursors of the (6-4) adduct of uracil and the corresponding adduct of thymine, shown as both ball and stick (top) and space-filling models (bottom)**.**

Table S1. ^{13}C chemical shifts for the major (6-4) adduct of uracil (**IIIa**) and the (6-4) adduct of thymine (**V**).

Please note: Wiley-Blackwell are not responsible for the content or functionality of any supporting information supplied by the authors. Any queries (other than missing material) should be directed to the corresponding author for the article.

REFERENCES

1. Cadet, J. and P. Vigny (1990) The photochemistry of nucleic acids. In *Bioorganic Photochemistry*, Vol. 1 (Edited by H. Morrison), pp. 1–272. John Wiley and Sons, New York.
2. Ruzsicska, B. P. and D. G. E. Lemaire (1995) DNA photochemistry. In *CRC Handbook of Organic Photochemistry and Photobiology* (Edited by W. M. Horspool and P.-S. Song), pp. 1289–1315. CRC Press, Boca Raton, FL.
3. Cadet, J., S. Courdavault, J.-L. Ravanat and T. Douki (2005) UVB and UVA radiation-mediated damage to isolated and cellular DNA. *Pure Appl. Chem.* **77**, 947–961.
4. Cadet, J., E. Sage and T. Douki (2005) Ultraviolet radiation-mediated damage to cellular DNA. *Mutat. Res.* **571**, 3–17.
5. Gordon, M. P., C.-W. Huang and J. Hurter (1976) Photochemistry and photobiology of ribonucleic acids, ribonucleoprotein, and RNA viruses. In *Photochemistry and Photobiology of Nucleic Acids*, Vol. 2 (Edited by S. Y. Wang), pp. 265–308. Academic Press, New York.
6. Zhirnov, O. V. and P. Wollenzien (2003) Action spectra for UV-light induced RNA-RNA crosslinking in 16S ribosomal RNA in the ribosome. *Photochem. Photobiol. Sci.* **2**, 688–693.
7. Smirnov, Y. A., S. P. Kapitulex and N. V. Kaverin (1992) Effects of UV-irradiation upon Venezuelan equine encephalomyelitis virus. *Virus Res.* **22**, 151–158.
8. Fisher, G. J. and H. E. Johns (1976) Pyrimidine photodimers. In *Photochemistry and Photobiology of Nucleic Acids*, Vol. 1 (Edited by S. Y. Wang), pp. 225–294. Academic Press, New York.
9. Fisher, G. J. and H. E. Johns (1976) Pyrimidine photohydrates. In *Photochemistry and Photobiology of Nucleic Acids*, Vol. 1 (Edited by S. Y. Wang), pp. 169–224. Academic Press, New York.
10. Davies, R. J. H. (1995) Ultraviolet radiation damage in DNA. *Biochem. Soc. Trans.* **23**, 407–418.
11. Shetlar, M. D., V. J. Basus, A. M. Falick and A. Mujeeb (2004) The cyclobutane dimers of 5-methylcytosine and their deamination products. *Photochem. Photobiol. Sci.* **10**, 968–979.
12. Moore, A. M. (1959) Ultraviolet irradiation of pyrimidine derivatives. III. Effect of HCN on the photolysis. *Can. J. Chem.* **37**, 1281–1287.
13. Shetlar, M. D. (1980) Cross-linking of proteins to nucleic acids by ultraviolet light. *Photochem. Photobiol. Rev.* **5**, 105–197.
14. Saito, I. and H. Sugiyama (1990) Photoreactions of nucleic acids and their constituents with amino acids and related compounds. In *Bioorganic Photochemistry*, Vol. 1 (Edited by H. Morrison), pp. 317–340. John Wiley and Sons, New York.
15. Hom, K., G. Strahan and M. D. Shetlar (2000) Ring opening photoreactions of cytosine and uracil with ethylamine. *Photochem. Photobiol.* **71**, 243–253.
16. Varghese, A. J. (1974) Photoaddition products of uracil and cysteine. *Biochim. Biophys. Acta* **374**, 109–114.
17. Smith, K. C. (1969) Photochemical addition of amino acids to ^{14}C-uracil. *Biochem. Biophys. Res. Commun.* **34**, 354–357.
18. Shetlar, M. D., J. Carbone, E. Steady and K. Hom (1984) Photochemical addition of amino acids and peptides to polyuridylic acid. *Photochem. Photobiol.* **39**, 141–144.
19. Wang, S. Y. (1976) Pyrimidine bimolecular photoproducts. In *Photochemistry and Photobiology of Nucleic Acids*, Vol. 1 (Edited by S. Y. Wang), pp. 295–356. Academic Press, New York.
20. Khattack, M. C. and S. Y. Wang (1969) Uracil photoproducts from uracil irradiated in ice. *Science* **163**, 1341–1342.
21. Varghese, A. J. (1971) Photochemistry of uracil and uridine. *Biochemistry* **10**, 4282–4290.
22. Taguchi, H. and S. Y. Wang (1976) Preparation and stereoconfigurations of heterodimers of pyrimidines. *Biochem. Biophys. Res. Commun.* **73**, 356–363.
23. Taguchi, H. and S. Y. Wang (1977) C-Alkylation and deterium exchange of cyclobutane-dipyrimidines. *J. Org. Chem.* **42**, 3321–3323.
24. Elad, D., I. Rosenthal and S. Sasson (1971) Solution photodimerization of 1,3-dimethyluracil. *J. Chem. Soc. (C)* 2054–2057.
25. Blackburn, G. M. and R. J. H. Davies (1966) The photochemistry of 1-methylthymine and 3-methylthymine. *J. Chem. Soc. (C)* 1342–1345.
26. Weinblum, D., F. P. Ottensmeyer and G. F. Wright (1968) The structures of the isomeric thymine dimers as deduced from their dipole moments. *Biochim. Biophys. Acta* **115**, 24–31.
27. Jennings, B. H., S. Pastra-Landis and J. W. Lerman (1972) Photosensitized dimerization of uracil. *Photochem. Photobiol.* **15**, 479–491.
28. Varghese, A. J. (1975) Photocycloaddition of acetone to uracil and cytosine. *Photochem. Photobiol.* **21**, 147–151.
29. Varghese, A. J. and S. Y. Wang (1968) Thymine-thymine adduct as a photoproduct of thymine. *Science* **160**, 186–187.
30. Wang, S. Y. (1971) Thymine phototrimer. *J. Amer. Chem. Soc.* **93**, 2768–2771.

31. Becker, E. D. (1980) *High Resolution NMR: Theory and Chemical Applications*, 2nd edn. Academic Press, Orlando, FL.
32. Bergstrom, D. E. and N. J. Leonard (1972) Photoreaction of 4-thiouracil with cytosine. Relation to photoreactions in Escherichia coli transfer ribonucleic acids. *Biochemistry* **11**, 1–9.
33. Karle, I. L. (1969) Crystal structure of a thymine-thymine adduct from irradiated thymine. *Acta Crystallogr. B* **25**, 2119–2126.
34. Smith, M. B. and J. March (2007) *March's Advanced Organic Chemistry: Reactions, Mechanisms and Structure*, 6th edn. John Wiley and Sons, Inc., New York.
35. Perrin, D. D. and B. Dempsy (1974) *Buffers for pH and Metal Ion Control*. Chapman and Hall, London, UK.
36. Hehre, W. and S. Ohlinger (2008) *Spartan '08 for Windows, Macintosh and Unix*. Wavefunction, Inc., Irvine, CA.
37. Montenay-Garestier, T., M. Charlier and C. Hélène (1976) Aggregate formation, excited-state interactions and photochemical reactions in frozen aqueous solutions of nucleic acid constituents. In *Photochemistry and Photobiology of Nucleic Acids*, Vol. 1 (Edited by S. Y. Wang), pp. 381–417. Academic Press, New York.
38. Rahn, R. O. and L. Hosszu (1969) Photochemical studies of thymine in ice. *Photochem. Photobiol.* **10**, 131–137.
39. Rhoades, D. F. and S. Y. Wang (1970) Uracil-thymine adduct from a mixture of uracil and thymine irradiated with ultraviolet light. *Biochemistry* **9**, 4416–4420.
40. Wang, S. Y. (1961) Photochemical reactions in frozen solution. *Nature* **190**, 690–694.
41. Smietanowska, A. and D. Shugar (1961) Photochemistry of model oligo- and polynucleotides. V. Properties of photodimers of uracil and thymine. *Bull. Acad. Polon. Sci. Cl. II* **9**, 375–380.
42. Wacker, A., D. Weinblum, L. Träger and Z. H. Moustafa (1961) Photochemical reactions with uracil and uridine. *J. Mol. Biol.* **3**, 790–793.
43. Smith, K. C. (1963) Photochemical reactions of thymine, uracil, uridine, cytosine and bromouracil in frozen solution and in dried films. *Photochem. Photobiol.* **2**, 503–517.
44. Blackburn, G. M. and R. J. H. Davies (1966) The structure of uracil photo-dimer. *Tetrahedron Lett.* **7**, 4471–4475.
45. Adman, E., M. P. Gordon and L. H. Jensen (1968) Structure of the *cis-syn*-photodimer of uracil: A puckered cyclobutane. *Chem. Commun.* 1019–1020.
46. Dönges, K. H. and E. Fahr (1966) The action of irradiation on nucleic acid components. IV. Structure of dimeric uracil formed by ultraviolet radiation of uracil. *Z. Naturforsch. B* **21**, 87.
47. Konnert, J., J. W. Gibson, I. L. Karle, M. N. Khattack and S. Y. Wang (1970) Crystal structure of dimers of uracil and 6-methyluracil. *Nature* **227**, 953–954.
48. Krauch, C. H., D. M. Kramer, P. Chandra, P. Mildner, H. Feller and A. Wacker (1967) Photodimerization of uracil sensitized by acetone. *Angew. Chem. Int. Ed. Engl.* **6**, 956.
49. Greenstock, C. L. and H. E. Johns (1968) Photosensitized dimerization of pyrimidines. *Biochem. Biophys. Res. Commun.* **30**, 21–27.
50. Richter, P. and E. Fahr (1969) Synthesis of *trans/syn*- and *trans/anti*-dimeric uracil. *Angew. Chem. Internat. Edit.* **8**, 208–209.
51. Richter, P. and E. Fahr (1970) Die synthese des *cis/syn*- und *cis/anti*-dimeren uracils. *Tetrahedron Lett.* **11**, 1921–1923.
52. Pasto, D. J. and C. R. Johnson (1969) *Organic Structure Determination*. Prentice-Hall, Englewood Cliffs, NJ.
53. Greenstock, C. L., I. H. Brown, J. W. Hunt and H. E. Johns (1967) Photodimerization of pyrimidine nucleic acid derivatives in aqueous solution and the effect of oxygen. *Biochem. Biophys. Res. Commun.* **27**, 431–436.
54. Brown, I. H. and H. E. Johns (1968) Photochemstry of uracil. Intersystem crossing and dimerization in aqueous solution. *Photochem. Photobiol.* **8**, 273–286.
55. Fendler, J. H. and G. Bogan (1974) Micellar effects on uracil photodimerization. *Photochem. Photobiol.* **20**, 323–328.
56. Lamola, A. A. and J. P. Mittal (1966) Solution photochemistry of thymine and uracil. *Science* **154**, 1560–1561.
57. Wagner, P. J. and D. J. Bucheck (1970) Photodimerization of thymine and uracil in acetonitrile. *J. Amer. Chem. Soc.* **92**, 181–185.